Predictive Control Methods for a 3-ϕ Induction Motor Drive

A Project Report

submitted by

KUNAL DAS

in partial fulfilment of the requirements
for the award of the degree of

BACHELOR OF TECHNOLOGY & MASTER OF TECHNOLOGY

DEPARTMENT OF ELECTRICAL ENGINEERING
INDIAN INSTITUTE OF TECHNOLOGY MADRAS.

MAY 2018

CERTIFICATE

This is to certify that the report titled **Predictive Control Methods for a 3-ϕ Induction Motor Drive**, submitted by **Kunal Das**, to the Indian Institute of Technology, Madras, for the award of the degree of **Master of Technology**, is a bona fide record of the research work done by him under my supervision. The contents of this report, in full or in parts, have not been submitted to any other Institute or University for the award of any degree or diploma.

Dr. Srirama Srinivas
Guide
Associate Professor
Dept. of Electrical Engineering
IIT-Madras, 600 036

Place: Chennai

Date: 12th May 2018

ACKNOWLEDGEMENTS

I am greatly indebted to **Dr. Srirama Srinivas**, from the Department of Electrical Engineering, Indian Institute Of Technology, Madras for his invaluable guidance through out the period of this project work. But for his kind encouragement and constant support, this project would not have been successfully completed.

I am also extremely grateful to **Mr. Nagasurya Prakash Musunuru** for his very useful suggestions and help in all the matters concerning the project, whenever sought by me. I also express my sincere thanks to **Mr. Pallab Sarkar, Mrs. N. Pratibha** and all others who have played a pivotal role in helping in the completing of this project.

I would be failing in my duty if I forget to express my gratitude to all the staff of the Machine's laboratory for their continuous cooperation while executing the project.

Finally I wish to take this opportunity to express my gratitude to **Ms. Komal Goel** for her constant support and encouragement throughout the entire duration of the project. I would also like to thank all those who have directly or indirectly, contributed in one way or the other to the success of this project.

(**KUNAL DAS**)

ABSTRACT

KEYWORDS: Induction motor; speed control of IM; V/f control; predictive control; model predictive control; PCC; PTC; M^2PC.

Predictive control is a class of controllers that have found application in the control of power converters and also motor drives after the need for advance control strategies. Research on this topic has been increased in the past few years due to the availability of advanced controller platforms needed for implementing the control. In this report, the application of different predictive control methods to power electronics and drives is presented. A simple classification of the most important types of predictive control is introduced, and each method is explained. Predictive control presents several advantages that make it suitable for the control of power converters and motor drives. Amongst this, model predictive control stands out and two of its most popular strategies, Predictive Current Control(PCC) and Predictive Torque Control(PTC), are also discussed in this report.

Model-based predictive direct control methods are advanced control strategies in the field of power electronics and motor drives. To control an induction machine (IM), the predictive torque control (PTC) method evaluates the electromagnetic torque and stator flux in the cost function. The switching vector selected for the inverter drive minimizes the error between the reference and predicted values. The system constraints can also be easily included. The predictive current control (PCC) strategy assesses the stator current in the cost function. Both the PTC and PCC methods are very useful direct control

methods that do not require the use of a modulator.

Traditional finite-set model predictive control (FSMPC) techniques are characterized by a variable switching frequency which causes noise as well as large voltage and current ripple. To overcome this, a novel predictive control strategy with a fixed switching frequency for a voltage source inverter called as modulated model predictive control (M^2PC) is proposed, with the aim of obtaining a modulated waveform at the output of the converter. The feasibility of this strategy is evaluated using simulation results to demonstrate the advantages of predictive control, in terms of fast dynamic response and the easy inclusion of nonlinearities. Finally, an optimized algorithm for this method is also introduced to minimize the cost function faster, with the constraints of the system maintained same, the performance of the system in terms of power quality is improved when compared to the same with the use of conventional control algorithm.

In this report, the PTC, PCC and M^2PC methods are discussed. The performance of all the control algorithms are tested on a 2-level inverter fed 3-ϕ induction motor drive . The behaviors and the robustness in steady state and the performances in transient state are also evaluated.

TABLE OF CONTENTS

LIST OF TABLES

LIST OF FIGURES

ABBREVIATIONS

AC	Alternating Current
DC	Direct Current
DSP	Digital Signal Processor
DSPC	Direct Speed Predictive Control
DTC	Direct Torque Control
EMF	Electro Motive Force
FOC	Field Oriented Control
IGBT	Insulated Gate Bipolar Transistor
IM	Induction Machine
MPC	Model Predictive Control
M^{2}PC	Modulated Model Predictive Control
PCC	Predictive Current Control
PI	Proportional Integral
PWM	Pulse Width Modulators
PTC	Predictive Torque Control
SPWM	Sine Pulse Width Modulation
SVM	Space Vector Modulation
VSI	Voltage Source Inverter

CHAPTER 1

Introduction

A.C.motor drive systems have varied uses in the modern industrial era and the catalyst for this are the cost, size, reliability and efficiency advantages carried by the induction motors. While the A.C. induction motor has many desirable advantages, the cost and complexity of the controller are few of the technical challenges one must endure while working with them. Pulse width modulators play a vital role in modern day power electronics and inverters utilize them to control frequency and voltage, maintain low harmonic content, and be compact and light weight. Inexpensive fast-switching PWM devices have gained wide acceptance in the power industry. As a result, a lot of thinking and research has been put to use to improve the methods of controlling the gate signals of the switches in the inverters. While advances in microelectronics technology is playing a vital role in reducing cost and complexity, research is still being undertaken to control the motor through various algorithms to set the duty cycle for the PWMs .
In this report, advanced control algorithms, starting with a description of Predictive control and evaluation of two of the most popular predictive control techniques i.e, PCC and PTC, followed by an optimized approach for M^2PC of the induction motor will be discussed as they are the focus of the present report.

1.1 Induction Motor

Induction Motor is commonly referred to as the "Workhorse of the Industry" due to its wide usage and applicability Its applications have gained importance in the fields of

transportation, industries, household appliances and laboratories, all of which are fueled by the use of induction motor in its very crux. The major reasons behind the wide usage of the Induction Motor are:

1. In the age cut throat competition, the prime requirement for any machine is to be cost effective and induction motors in comparison to DC and synchronous motors do just that. Due to its economy of procurement, installation and use, the induction motor is usually the first choice for any operation in any power field.
2. Their sturdy construction and robustness enable them to be used in all kinds of environments that too for long periods.
3. Efficiency and reliability can be considered synonymous to induction machine.
4. Owing to its ease of construction, induction motors demand a very low maintenance costs.
5. Induction Motor has a very high starting torque, which help in applications of load application before starting the motor.

Adding to the list, the speed of an induction motor can be controlled with ease. Different applications require different required speeds for the motor to run at. At such instances, speed control becomes more of a necessity as:

1. It ensures smooth operation.
2. It provides torque and acceleration control.
3. It compensates for fluctuating process parameters.

1.2 Speed Control methods of Induction Motor Drive

Various methodologies can be opted to control the speed of an induction motor, which include:

1. Variable Frequency Control
2. Stator Voltage Control
3. Variable Rotor Resistance Control
4. Slip Recovery
5. V/f Control

1.2.1 Variable Frequency Control

Variable Frequency Control is a method in which the synchronous speed and therefore, the speed of the motor can be controlled by varying the supply frequency. The synchronous speed of an induction motor is given by the relation:

$$N_s = 120 * f/p$$

The EMF induced in the stator of the induction motor is related to the torque as:

$$E_1 = 4.44 * K_W * f * \psi * T_1$$

So, if the supply frequency changes, induced EMF must also change to maintain the same air gap flux. The terminal voltage V_1 is almost equal to the induced EMF E_1 if the stator voltage drop is neglected.
To minimize losses and to avoid saturation, the motor is operated at rated air gap flux. This condition is obtained by varying the terminal voltage with frequency so as to maintain a constant (V/f) ratio fixed to the rated value. This type of control is known as

Constant Volts Per Hertz control. Hence, this calls for the need of a variable power source to control the speed of an induction motor using variable frequency control.
The variable frequency control allows good running and transient performance that need to be taken from a squirrel cage induction motor. Cyclo converter controlled induction motor drive is suitable only for large power drives and to get lower speeds.

1.2.2 Stator Voltage Control

In the process of stator voltage control, the speed of a three phase induction motor is varied by varying the supply voltage. The torque developed is proportional to the square of the supply voltage and the slip at the maximum torque is independent of the supply voltage and dependent on rotor resistance. The variation in the supply voltage does not alter the synchronous speed of the motor. This can be well visualized with the help of speed-torque characteristics for a load. In this case the load taken is an fan load as seen in the Fig. 1.1.

By varying the stator voltage, the speed can be controlled. The voltage is varied until the torque required by the load is developed, at the desired speed. The torque developed is proportional to the square of the supply voltage and the current is proportional to the voltage.
Hence, to reduce the speed for the same value of the current, the value of the voltage is reduced and as a result, the torque developed by the motor is reduced. This stator voltage control method is suitable for the applications where the load torque also decreases with the speed as is the case with the fan load.
This method gives a speed control only below the rated speed as the operation of the voltages if higher than the rated voltage, is not permitted. This method is suitable where the intermittent operation of the drive is required. The load torque varies as the square of the speed. These types of drives require low torque at lower speeds. This condition

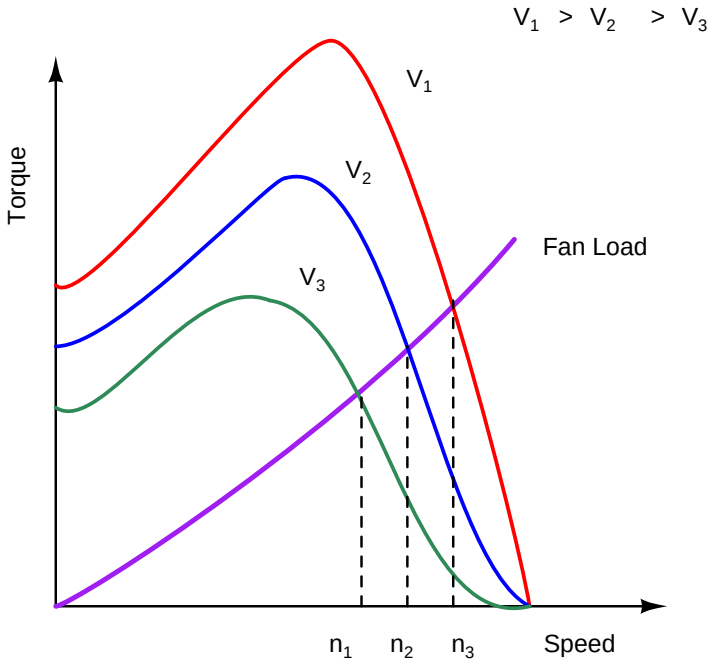

Fig. 1.1: Speed-Torque characteristics with variable stator voltage.

can be obtained by applying lower voltage without exceeding the motor current.

1.2.3 Variable Rotor Resistance Control

Rotor Resistance Control is also one of the methods by which, the speed of the Induction motor can be controlled. The speed of the wound induction motor can be controlled by connecting an external resistance in the rotor circuit through slip rings. This method is not applicable to cage rotor induction motor.

The torque equation is given as:

$$T = \frac{sE_r^2 R_r}{R_r^2 + (sX_r)^2} * \frac{3}{2\pi n_s} \tag{1.1}$$

For maximum torque, $\frac{dT}{ds} = 0$. On solving it, maximum slip at which maximum torque is obtained and the maximum torque itself can be obtained as given below:

$$s_{max} = \frac{R_r}{X_r} \tag{1.2}$$

$$T_{max} = \frac{3}{2\pi n_s} \frac{E_r^2}{2X_r} \tag{1.3}$$

As we can see that the maximum torque is independent of the rotor resistance R_r, yet the slip at which the maximum torque τ_{max} is available is dependent on it. The larger the value of the resistance, larger will be the value of the slip at which the maximum torque occurs. If the resistance of the motor is increased, then the pull out speed of the motor decreases. But the maximum torque remains constant. Thus, by Rotor Resistance Control method, the speed control is provided from the rated speed to the lower speeds. This method of speed control is very simple. It is possible to have a large starting torque, low starting current and large values of the pullout torque at a small value of slip.

The flip side of the rotor resistance control method is that the efficiency is low because of the additional losses due to the resistors connected in the rotor circuit. The efficiency is greatly reduced at low speeds because of the higher value of the slip. This method of speed control is used in cranes and other intermittent load applications because of the low cost and high torque capability at the lower speed.

This speed control method can also be used in fans or pump drives, where speed variation over a small range near the maximum or top speed is required.

1.2.4 Slip Recovery

Slip Energy Recovery is one of the methods of controlling the speed of an induction motor. This method is also known as Static Scherbius Drive. In the rotor resistance control method, the slip power in the rotor circuit is wasted as I^2R losses during the

low-speed operation, thereby the efficiency is reduced. The slip power from the rotor circuit can be recovered and fed back to the AC source so that it can be utilized outside the motor. Thus, the overall efficiency of the drive system can be increased.

The basic principle of the slip power recovery is to connect an external source of the EMF of the slip frequency of the rotor circuit. The slip energy recovery method provides the speed control of a slip ring induction motor below its synchronous speed. A portion of rotor AC power (slip power) is converted into DC by a diode bridge.

The smoothing reactor is provided to smoothen the rectified current. The output of the rectifier is then connected to the DC terminals of the inverter. The inverter inverts the DC power to the AC power and feeds it back to the AC source. The inverter is a controlled rectifier operated in the inversion mode.

This method of speed control is used in large power applications where the variation of speed over a wide range involves a large amount of slip power.

1.2.5 V/f Control

The operation of induction motors in the so-called constant volts per hertz (V/f) mode has been known for many decades, and its principle is well understood [1]. With the introduction of solid-state inverters, the constant V/f control became popular [2], [3], [4], and the great majority of variable speed drives in operation today are of this type. However, since the introduction of vector control theory, almost all research has been concentrated in this area, rather than constant V/f operation. Its practical application at low frequency is still challenging, due to the influence of the stator resistance and the necessary rotor slip to produce torque. In addition, the nonlinear behavior of the modern pulsewidth modulated voltage-source inverter (PWMVSI) in the low voltage range c, [5], [6] makes it difficult to use constant V/f drives at frequencies below 3 Hz [7].The simplest stator resistance compensation method consists of boosting the stator

voltage by the magnitude of the current-resistance (IR) drop. A vector compensation was proposed, but it required both voltage and current sensors and accurate knowledge of machine inductances. More recently, a scalar control scheme was proposed. In this scheme, the flux magnitude is derived from the current estimation. In [8], using the dc-link voltage and current, both flux and torque loops are introduced. Its use at low frequency is limited by the flux estimation. Also, the slip compensation was based on a linear torque-speed assumption which led to large steady-state errors in speed for high load torques. A linearized frequency compensation control based on an "ideal induction motor" was proposed in [9].

The various advantages of V/f Control are as follows:

1. It provides good range of speed.
2. It gives good running and transient performance.
3. It has low starting current requirement.
4. It has a wider stable operating region.
5. Voltage and frequencies reach rated values at base speed.
6. The acceleration can be controlled by controlling the rate of change of supply frequency.

1.3 Motivation: The need of an advanced control strategy

Different types of speed control methods discussed above generally refer to open-loop control. In such control stratergies, a sequence of input signals are computed which steer the given system. However, if the input sequence is applied to the real system, there is usually a deviation between the predicted an actual behavior due to system-model mismatch and disturbances. So this deviation has either to be accepted or combine these

control strategies with a closed-loop method. This marked the need of an advanced control method which gave birth to the predictive control strategies, mainly MPC, which is a closed-loop control.

In MPC, the correction is built in, so as to recompute the optimal sequence after periodically resetting the initial conditions in the MPC problem to the true state of the system (or an estimation thereof). The varied advantages and the effective performance were the primary motivation to work and enumerate more in this area while diving into the further aspects of this control and its major applications, primarily in the predictive control strategies

In the following chapters, various kinds of advanced converter control is introduced and the wider applicability of predictive control over other forms are discussed . This will act as the literature review for the comparison of predictive current control and predictive torque control and will give an insight on how the proposed algorithm for modified model predictive control betters the conventional algorithm.

CHAPTER 2

Predictive Control

2.1 Introduction

In chapter 1, various open-loop optimal speed control strategies and its applicability in the present day, were discussed. The flaws of these control strategies and the deviation of the predictive behavior from the actual behavior acted as the catalyst for the development of an advanced control strategy, which eventually gave rise to the predictive control strategies This chapter presents the different strategies of predictive control that are used even today.

The use of power converters has become very popular in the recent decades for a wide range of applications, including drives, traction, and distributed generation etc. The control of power converters has been extensively studied, and new control schemes are introduced every year. Several control schemes have been proposed for the control of power converters and drives. Some of them are shown in Fig. 2.1.

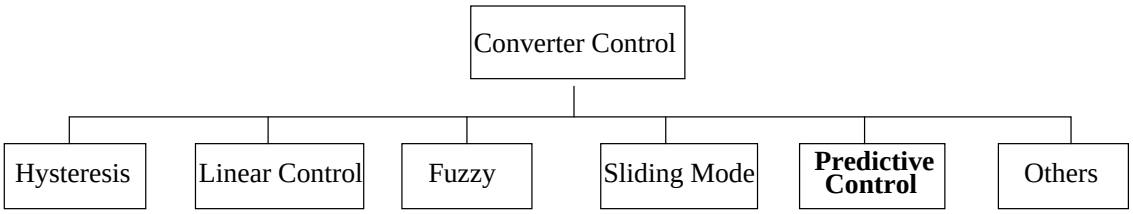

Fig. 2.1: Basic methods of converter control.

Amongst these, hysteresis and linear controls with pulsewidth modulation (PWM) are

the most established in the literature. However, with the development of faster and more powerful microprocessors, new and more complex control schemes have emerged. Some of these new control schemes for power converters include fuzzy logic, sliding mode control, and predictive control. Fuzzy logic is suitable for applications where the controlled system or some of its parameters are unknown. Sliding mode control presents robustness and takes into account the switching nature of the power converters. Other control schemes found in the literature include neural networks, neuro fuzzy, and other advanced control techniques.

Predictive control presents several advantages over the others that make it suitable for the control of power converters:

1. concepts are intuitive and easy to understand
2. it can be applied to varied systems
3. constraints and nonlinearities can be easily included
4. multivariable cases can be considered and
5. the resulting controller is easy to implement.

It requires higher amount of calculations, when compared to a classic control scheme. However, the fast microprocessors available today makes the implementation of predictive control, easier. Generally, the quality of the controller depends on the quality of the model. This chapter gives a brief idea of the important types of predictive control methods applied to the power electronics and drives. A classification of them is presented in Section II, and each type of predictive control is explained thereafter. Hysteresis-based predictive control is presented in Section III, trajectory-based predictive control in Section IV, deadbeat control in Section V and finally model predictive control (MPC) in Section VI.

2.2 Classification of Predictive Control Methods

Recently, Predictive control have found application in power converters due to its very wide variety of controllers. The classification of different predictive control methods is shown in Fig. 2.2.

The main idea of predictive control is to predict the future behavior of the controlled variables of the model of the system used. This information is used by the controller in order to obtain the optimal actuation, according to a predefined optimization criteria.

The optimization criteria is different for different methodologies. For example, in the hysteresis-based predictive control, the idea is to keep the controlled variable within the boundaries of a hysteresis area, while in the trajectory based, the variables are forced to follow a predefined trajectory. In deadbeat control, the optimal actuation makes the error equal to zero in the next sampling instant. A more flexible criteria is used in MPC, expressed as a cost function that has to be minimized.

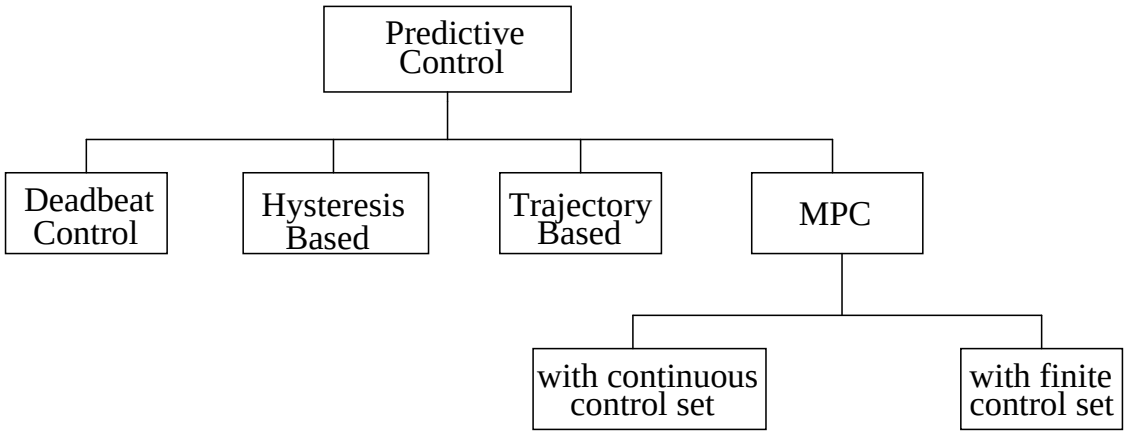

Fig. 2.2: Classification of predictive control methods used in power electronics.

One advantage of predictive control is that concepts are very simple and intuitive. Depending on the type of predictive control, its implementation is also simple, as with deadbeat control and finite control set MPC (FS-MPC), particularly for a two-level converter with horizon N = 1 [10]. However, in general, some implementations of MPC can be more complex. Variations of the basic deadbeat control, to make it more sturdy, can also become very complex and make it both difficult to understand and also to implement.

Using predictive control, it is possible to avoid the cascaded structure, used primarily in a linear control scheme, obtaining very fast transient responses. Nonlinearities of a system can be included in the model, avoiding the need of linearizing the model for given operating points and improving the operation of the system for all conditions. It is also possible to include restrictions to some variables while designing the controller. An overview of each type of predictive control is presented in the following sections.

2.3 Hysteresis Based Predictive Control

Hysteresis-based predictive control strategies try to keep the controlled system variables between the boundaries of a hysteresis area or space. The most simple form of this principle is the "bang bang controller." An improvised form of a bang bang controller is the predictive current controller. The block diagram of the hysteresis-based predictive control is shown in Fig. 2.3.

Using PCC, the switching instants are determined by suitable error boundaries. For example, Fig. 2.4 shows a circular boundary, the location of which is controlled by the current reference vector I_s^*. When the current vector touches the boundary line, the next switching state vector is determined through prediction and optimization. The trajectories of the current vector for each possible switching state are computed, and

then predictions are made for the respective time intervals required to reach the error

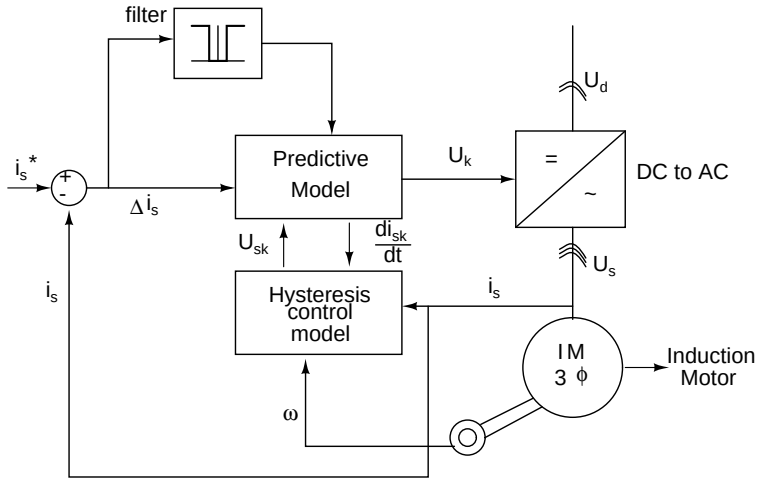

Fig. 2.3: Hysteresis based predictive control

boundary again. Thus, the loop keeps running until required. These events also depend on the location of the error boundary, which is considered moving in the complex plane as commanded by the predicted current reference. The movement is indicated by the dotted arc in Fig. 2.4.

The maximum possible switching frequency is limited by the computing time of the algorithms which determine the optimal switching state vector. Higher frequencies can also be handled by employing the double prediction method. Well before the boundary is reached, the actual current trajectory is predicted in order to identify the time instant at which the boundary transition is likely to occur.

The back EMF vector at this time instant is then predicted. It is used for the optimal selection of the future switching state vector using the earlier described methodology. A further reduction of the switching frequency, which may be needed in very high-power applications, can be achieved by defining a current error boundary of rectangular shape,

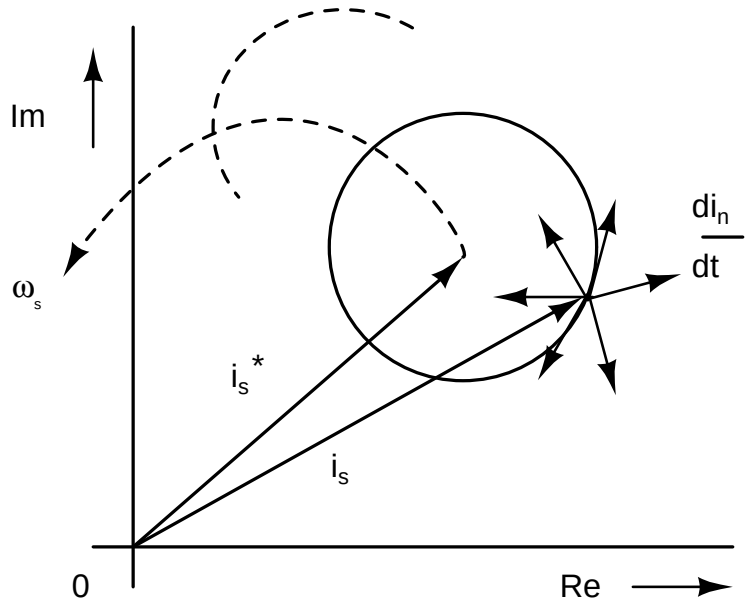

Fig. 2.4: Hysteresis based predictive control

having the rectangle aligned with the rotor flux vector of the machine.
Using field-oriented predictive current control, the switching frequency can be reduced more than with a circular boundary area in stator coordinates [11]. Today, different optimizing criteria are considered, modifications of the predictive current control are consequently under scrutiny and is being worked upon.

2.4 Trajectory Based Predictive Control

The principle of trajectory-based predictive control strategies is to force the system's variables onto pre calculated trajectories. Control algorithms according to this strategy are direct self control [12] or direct mean torque control. Other methods like sliding mode control or direct torque control [13] are a combination of hysteresis and trajectory-based strategies, whereas direct speed predictive control (DSPC) can be identified as a

trajectory-based control system, even though it has a few hysteresis-based aspects. Unlike cascade controllers, predictive control algorithms offer the possibility to directly control the desired system values. Most predictive control methods published so far only deal with stator currents, torque, or flux (linear) directly; the drive speed is controlled by a superimposed control loop. In contrast,DSPC shown in Fig. 2.5, in contrast, has no control loop of this type; the switching events in the inverter are calculated in a way where speed is directly controlled in a time saving manner.

Similar to the methods mentioned above, the switching states of the inverter are classi-

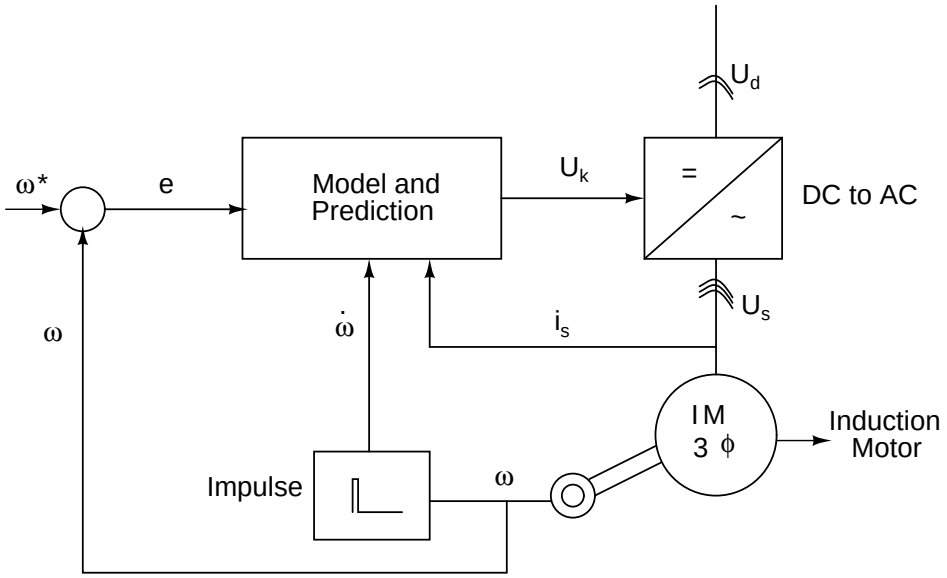

Fig. 2.5: Direct Speed Predictive Control

fied as "torque increasing," "slow torque decreasing," or "rapid torque decreasing." For small time intervals, the inertia of the system and the derivatives of machine and load torques are assumed as constant values. The behavior of the system leads to a set of parabolas in the speed error versus acceleration area as shown in Fig. 2.6

The initial state of the system is assumed to be e_k/a_k. In this state, a torque increasing voltage vector has to be produced by the inverter, and therefore, the switching state

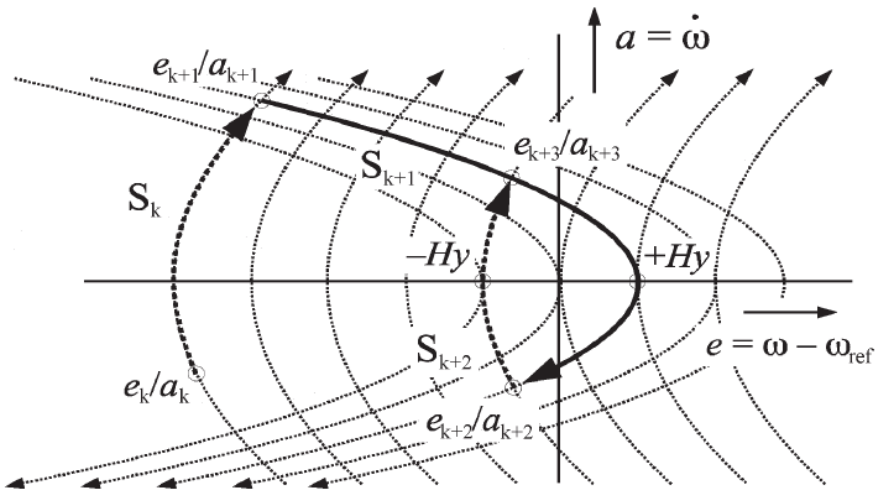

Fig. 2.6: Trajectory parabolas in the e/a state plane

S_k is chosen. The state now travels along the dotted parabola until the point e_{k+1}/a_{k+1} is reached. This is the intersection with another parabola for a "torque decreasing" switching state S_{k+1}, which will pass through the point " $+Hy$." The intersection e_{k+1}/a_{k+1} is pre calculated as the optimal switching instant to reach the desired state point " $+Hy$." at the earliest. Now, in e_{k+1}/a_{k+1}, the inverter is commutated into the switching state S_{k+1}. After this , the state of the system travels along the new parabola until the point e_{k+2}/a_{k+2} is reached. At this stage, the inverter is switched again into a torque increasing state S_{k+2}. The corresponding trajectory passes the point " $-Hy$." In steady state, the state moves along the path $+Hy - e_{k+2}/a_{k+2} - Hy - e_{k+3}/a_{k+3} - Hy$. Hence, the speed error 'e' is kept in the hysteresis band between $-Hy$ and $+Hy$. This is the hysteresis aspect of this strategy mentioned earlier. Of course, the optimal steady state point would be the point of origin.However, since the switching frequency of the inverter is limited, the drive state cannot be fixed to that point.

Therefore, the hysteresis band is defined to keep the switching frequency in an acceptable range. The algorithm of DSPC clearly shows the main principle of predictive con-

trol that the previous knowledge of the drive system is used to pre-calculate the optimal switching states instead of trying to linearize the nonlinear parts of the system and then control them by PI controllers. Thus the speed can be controlled directly without the need of a cascaded structure.

2.5 Deadbeat Based Predictive Control

This is a well-known type of predictive controller. This approach uses the model of the system to calculate the required reference voltage once every sampling period in order to reach the reference value in the next sampling instant. Then, this voltage is applied using a modulator. It has been applied for current control in three-phase inverters, rectifiers, active filters, power factor correctors, uninterruptible power supplies, dc dc converters, and torque control of induction machines. While this method has been used when a fast dynamic response is required, being deadbeat-based, it is often fragile. Errors in the parameter values of the model, unmodeled delays and other errors in the model often deteriorate the system performance and may even give rise to instability. Another disadvantage of these deadbeat control schemes is that non linearities and constraints of the system variables are difficult to incorporate.

2.5.1 Deadbeat Current Control

A typical deadbeat current control scheme is shown in Fig. 2.7. Compared to a classic current control scheme, here the PI controller has been replaced by the deadbeat controller. The reference voltage is applied using a modulator. The load model for a generic RLE load is described by the following space vector equation:

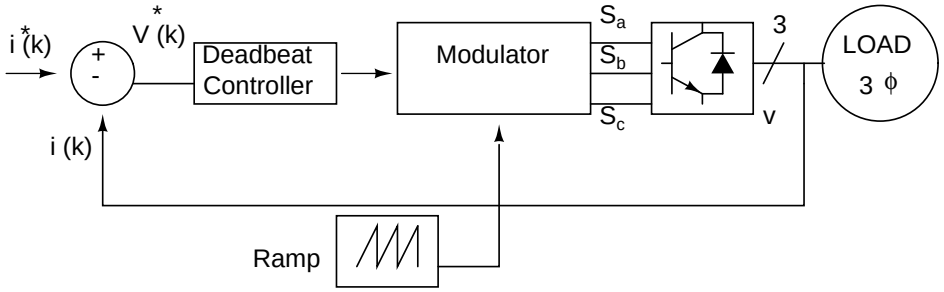

Fig. 2.7: Deadbeat Current Control

$$v = Ri + L\frac{di}{dt} + e \tag{2.1}$$

where v is the voltage space vector, i is the current space vector, and e is the EMF voltage space vector.

The following discrete-time equation can be obtained from (2.1) for a sampling time T_s:

$$\frac{1}{\delta}i(k+1) - \frac{\chi}{\delta}i(k) = v(k) - e(k) \tag{2.2}$$

where $\delta = e^{-T_s R/L}$ and $\chi = \frac{1}{R}(1 - e^{-T_s R/L})$. Based on the discrete-time model (2.2), the reference voltage vector is obtained as

$$v^*(k) = \frac{1}{\delta}[i^*(k+1) - \chi i(k)] + e(k). \tag{2.3}$$

Reference voltage v is applied in the converter using a modulator. The basic operating principle of deadbeat current control is shown in Fig. 2.8.

Here, the load current i at time k is different from the reference current i^*. This error is used for calculation of the reference voltage v^*, which is applied to the load at time k. Ideally, at time $k+1$, the load current will be equal to the reference current.

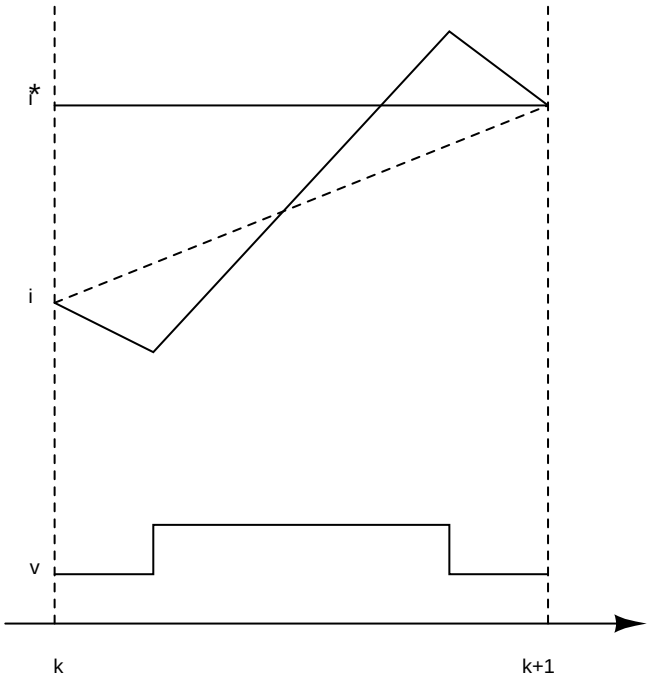

Fig. 2.8: Illustration of deadbeat current controller operation

2.5.2 Modifications to Basic Algorithm

When implemented in a real system, several problems may appear and deteriorate the performance of a deadbeat controller. One of them is the delay introduced by calculation time and modulation. This problem has been solved in [14], [15], and [16] by considering this delay in the model. Another important issue is the sensitivity to plant uncertainties and errors in the model parameter values. Several solutions to this problem have been proposed, including the use of an adaptive self-tuning scheme [17] , a predictive internal model [18], and neural networks [19].

In some applications, information about the disturbances is needed by the controller, and these include variables which are not measured. In these cases, the use of disturbance observers was proposed [20], [21]. Other specific applications can require a modified algorithm for reduced switching frequency, as proposed in [22].

2.6 Model Predictive Control

Model-based predictive control (MPC) for power converters and drives is a control technique that has gained a great deal of attention in the recent times. The main reason is that although MPC presents high computational burden, it can easily handle multivariable control functions, system constraints and nonlinearities in a very intuitive way. Taking advantage of that, MPC has been successfully used for different applications such as an active front end (AFE) converters, power converters connected to resistor inductor RL loads, uninterruptible power supplies, and highperformance drives for induction machines, among others.

2.6.1 The MPC Control Strategy

Predictive control is understood as a wide class of controllers; its main characteristic is the use of the model of the system for the prediction of the future behavior of the controlled variables over a prediction horizon, N. This information is used by the MPC control strategy to provide the control action sequence for the system by optimizing a user-defined cost function. It should be noted that the algorithm is executed again every sampling period and only the first value of the optimal sequence is applied to the system at instant k. The cost function can have any form, but it is usually defined as

$$g = \sum_{n=1} \lambda_i (x_i^* - x_i^p)^2 \tag{2.4}$$

where x_i^* is the reference command, x_i^p is the predicted value for variable x_i, λ_i is a weighting factor, and index i stands for the number of variables to be controlled. In this simple way, it is possible to include several control objectives (multivariable case),

constraints, and nonlinearities. The predicted values, x_i^p are calculated by means of the model of the system to be controlled.

2.6.2 System Model

Most MPC strategies are formulated in a discrete-time setting with a fixed sampling interval, for example, $h > 0$. Here, system inputs are restricted to change their values only at the discrete sampling instants, i.e., at times $t = kh$, where $k \in 0, 1, 2, ...$ denotes the sampling instants.A basic system model is presented in Fig. 2.9 Since power electronics applications are often governed by nonlinear dynamic relations, it is convenient to represent the system to be controlled in discrete-time state space form via

$$x(k+1) = f(x(k), u(k)), \qquad k \in 0, 1, 2, ... \tag{2.5}$$

where $x(k)$ denotes the state value at time k, whereas $u(k)$ is the plant input. Here the configurations of the controller output, feeds into a modulator stage providing the switching positions, consequently restricting the system inputs $u(k)$ in (2.5) according to

$$u(k) \in U \subseteq R^p, \qquad k \in 0, 1, 2, ... \tag{2.6}$$

where U is a polytopes and p denotes the number of switches. For example, the components of $u(k)$ could correspond to duty cycles or PWM reference signals, in which case, U is formed of intervals, namely, $U = [0, 1]^p$. Clearly, the mentioned model can only approximate switching effects. Nevertheless, several interesting proposals for power electronics and drives have been developed by using this simple setting. In addition to the constraints on the system inputs, MPC also allows one to incorporate state

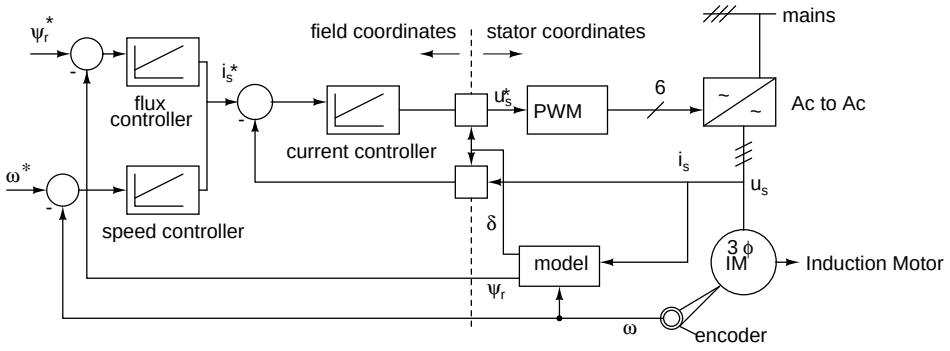

Fig. 2.9: Typical field-oriented control of an induction machine

constraints, for example

$$x(k) \in X \subseteq R^n, \qquad k \subseteq 0, 1, 2, ... \tag{2.7}$$

State constraints can correspond to constraints on capacitor voltages in flying capacitor converters or neutral point clamped converters. Constraints on inductive load currents can also be modeled as state constraints.

CHAPTER 3

Evaluation of PCC and PTC Methods

Direct torque control (DTC) method requires neither a modulator nor an internal current PI controller. These features make the system implementation easier and lead to a faster dynamic response as presented in [23], [24]. DTC method uses two independent hysteresis controllers; one for electromagnetic torque and other for the stator flux. In the controller design, a look-up-table (LUT) also must be built ahead of time for the direct output of the signals. With the same aim of realizing the direct control, predictive direct control methods have gained more attention during the past decade as alternative approach.

Predictive direct control methods belong to the family of model-based predictive control (MPC). The MPC method is an advanced control method in process industries. Continuous MPC methods need a modulator in the system design. However, predictive direct control methods incorporate the model of the applied inverter directly into the controller. All feasible inverter switching states are considered in order to minimize the cost function, which normally consists of the errors between reference and measured (or estimated) control variables and can also have additional functions. Finally, the switching state that minimizes the cost function is selected as the output signal during the next iteration. The cost function is very flexible and is totally dependent on the user on what parameters they would like to consider.

The design of the weighting factor in the cost function can be found in [25] and [26]. The most advanced developments of predictive direct control for power electronics are clearly presented in [27]. Among all available predictive direct control strategies for power electronics, **predictive current control (PCC) and predictive torque control**

(PTC) are the two most popular control methods. PCC method was first proposed in 2007 [28] . PCC was applied by using a resistance and inductance circuit (RL) load. The cost function only considers the errors between the current reference and the measured current. This novel method attracted the attention of the scientific community very quickly due to its straightforward algorithm and good performances both in steady and transient states, and since been widely applied. In the same year, the PTC method was proposed for the control of electrical drives [29]. In this method, the cost function takes the errors of electromagnetic torque and magnitude of the stator flux into consideration. The PTC method has proven to be a very promising control method for motors, and it even has comparable performances with those of the field oriented control (FOC) method.

In this report, the PTC and PCC methods are implemented and tested for an induction machine (IM) load using the same set of parameters. These experiments are developed for demonstrating the differences and similarities of the two methods. This chapter is organized in the order that Section 3.1 described the mathematical model of an IM and the voltage source inverter. In Section 3.2, the PTC and PCC methods are explained. Section 3.3 presents the results and explanation.

3.1 Models of an IM and inverter

To test a squirrel-cage IM for both the PCC and PTC methods, firstly the mathematical model of an IM in an appropriate reference frame is developed. The mathematical model of an IM can be described by a well-known set of complex equations in the stator reference frame as described below:

$$v_s = R_s.i_s + \frac{d}{dt}\psi_s \tag{3.1}$$

$$0 = R_r.i_r + \frac{d}{dt}\psi_r - j.\omega.\psi_r \tag{3.2}$$

$$\psi_s = L_s.i_s + L_m.i_r \tag{3.3}$$

$$\psi_r = L_r.i_r + Lm.i_s \tag{3.4}$$

$$T = \frac{3}{2}.p.Im(\psi_s^*.is) \tag{3.5}$$

where v_s denotes the stator voltage vector, ψ_s and ψ_r represent the stator flux and rotor flux, respectively. i_s and i_r are the stator and rotor currents. R_s and R_r are the stator and rotor resistances. L_s, L_r, and L_m are stator, rotor, and mutual inductance, respectively, and ω is the electrical speed. p is the number of pole pairs and T denotes the electromagnetic torque. In this report, a two-level voltage source inverter is used for both the PTC and PCC methods. The topology of the inverter and its feasible voltage vectors are presented in Fig. 3.1. The switching vector S can be expressed as:

$$S = \frac{2}{3}(S_a + \mathbf{a}S_b + \mathbf{a^2}S_c) \tag{3.6}$$

where $a = e^{j2/3}$, $S_i = 1$ means ON, $\overline{Si}$ means OFF, and $i = a, b, c$. The voltage vector v is related to the switching state S by

$$v = V_{dc}.S \tag{3.7}$$

where V_{dc} is the dc-link voltage of the inverter.

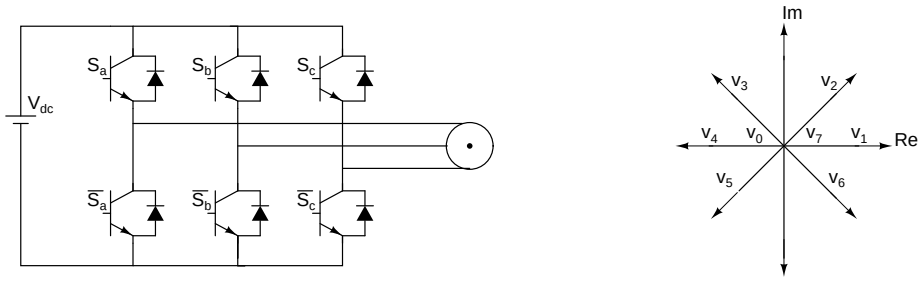

Fig. 3.1: Two-level voltage source inverter *(left)* and inverter voltage vectors *(right)*.

3.2 Predictive Control Methods for a 3-ϕ IM

3.2.1 PCC

With the PCC algorithm, the stator currents are predicted for all feasible voltage vectors, and then these predictions are evaluated in a cost function [28]. The one that minimizes the cost function will be selected for the optimal gate signals of the insulated gate bipolar transistors (IGBTs) of the inverter in the next sampling cycle. For long prediction steps, only the first voltage vector (corresponding to the next time step) of this optimal set is applied to the inverter referring to the receding horizon principle.

From the IM model described in Section 3.1, the stator current can be derived as shown:

$$i_s = -\frac{1}{R_\sigma}((L_\sigma.\frac{di_s}{dt} - k_r.(\frac{1}{\tau_r} - j.\omega).\psi_r) - v_s) \tag{3.8}$$

where $k_r = L_m/L_r, R_\sigma = R_s + k_r^2.R_r$ and $L_\sigma = \sigma.L_s$.

To predict the value in the next step, the forward Euler discretization is considered as given below:

$$\frac{dx}{dt} \approx \frac{x(k+1) - x(k)}{T_s} \tag{3.9}$$

where T_s is the sampling time of the system.
From (3.8) and (3.9), the stator current can be predicted as

$$\hat{i_s}(k+1) = (1 - \frac{T_s}{\tau_\sigma}).\mathbf{i_s}(k) + \frac{T_s}{\tau_\sigma}\frac{1}{R_\sigma}.[k_r.(\frac{1}{\tau_r} - j.\omega(k)).\psi_r(k) + \mathbf{v_s}(k)] \tag{3.10}$$

where $\tau_\sigma = \sigma.L_s/R_\sigma$. The classical cost function (g_j) is given as:

$$g_j = \sum_{h=1}^{N} |i_\alpha^* - i_\alpha(k+h)_j| + |i_\beta^* - i_\beta(k+h)_j| \tag{3.11}$$

where $j = 0, ..., 6$, as we are dealing with a two-level voltage source inverter in this system. All feasible voltage vectors are presented in Fig. 3.1. The inverter has eight different switching states but only seven different voltage vectors. Thus, the need to calcualte the cost function, only seven times. Therefore, g_j has seven different values. Among these values, the one that minimizes the g_j is selected as the output vector. h is the predictive horizon. In this case, only one step of PCC is considered,thus $h = 1$.

From (3.11), to complete the design of the PCC method, the generation of the current references is necessary. The block diagram of the PCC method is depicted in Fig. 3.2. The torque reference is generated by a speed PI controller, and the rotor flux reference is considered as a constant value. The corresponding reference values for the field- and torque-producing currents i_d^* and i_q^* are produced as given by:

$$i_d^* = \frac{|\psi_r|^*}{L_m} \tag{3.12}$$

$$i_q^* = \frac{2}{3}\frac{L_r}{L_m}\frac{T^*}{|\psi_r|^*} \tag{3.13}$$

In the cost function (g_j), the state's current values in $\alpha\beta$ frame are required. The inverse

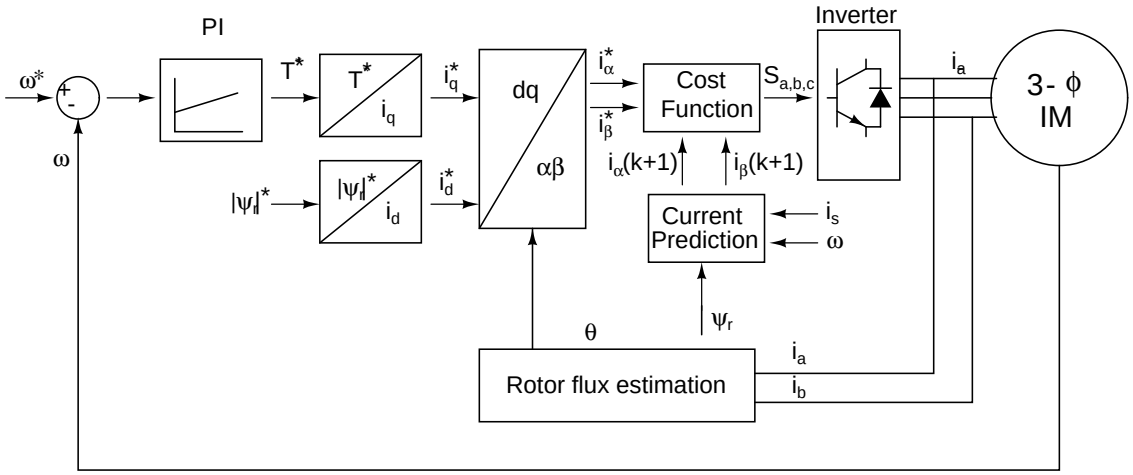

Fig. 3.2: Block diagram of PCC.

Park transformation is presented to satisfy this requirement as follows:

$$\begin{bmatrix} \alpha \\ \beta \end{bmatrix} = \begin{bmatrix} cos(\theta) & -sin(\theta) \\ sin(\theta) & cos(\theta) \end{bmatrix} \begin{bmatrix} d \\ q \end{bmatrix} \tag{3.14}$$

where θ is the rotating angle.

3.2.2 PTC

The architecture of the PTC method is shown in Fig. 3.3. The core aspects of PTC are the torque and flux predictions and these two parameters form the crux of the cost function.

In the PTC, the next-step stator flux $\hat{\psi}_s(k+1)$ and the electromagnetic torque $\hat{T}(k+1)$ must be calculated. By using (3.9) to discretize the voltage model (3.1), the stator

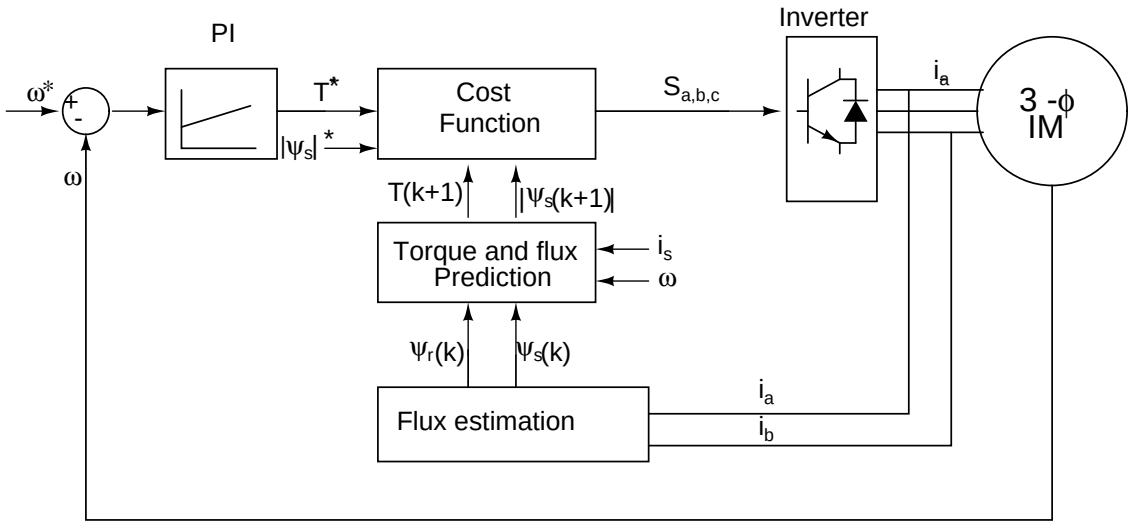

Fig. 3.3: Block diagram of PTC.

flux prediction can be obtained as:

$$\hat{\psi}_s(k+1) = \psi_s(k) + T_s.v_s(k) - R_s T_s i_s(k). \tag{3.15}$$

According to (3.5), with predictions of the stator flux in (3.15) and the predicted current in (3.10), the electromagnetic torque can be predicted as:

$$\hat{T}(k+1) = \frac{3}{2}.p.Im(\hat{\psi}_s(k+1)^*.\hat{\mathbf{i}}_\mathbf{s}(k+1)). \tag{3.16}$$

The classical cost function for the PTC method is given as:

$$g_j = \sum_{h=1}^{N} |T^* - \hat{T}(k+h)_j| + \lambda.|||\hat{\psi}_s^*|| - ||\hat{\psi}_s^*(k+h)_j|||| \tag{3.17}$$

3.3 Implementation and Results

To verify the effectiveness of the two methods, a simulation comparison in a MATLAB/Simulink environment is carried out.

3.3.1 Simulation results

The parameters of the main motor are mentioned in **Table 3.1**. For a proper equal comparison of the two methods i.e. PCC and PTC, the external PI speed controllers are configured with the same set of parameters.The sampling frequency is set at 100 kHz, which is the value of the test bench. The simulation test is carried out and the system behavior at four different conditions viz. starting response, steady state response, transient response and speed reversal response are noted. Both methods work at rated speed of 1435 rpm with a full load of 9.9818 N-m. During the test, the measured speed, the electromagnetic torque, and the stator current are observed. The simulation results of the PCC method and the PTC method at the start, in the steady state, the transient

Table 3.1: Parameters of the IM.

$Parameters$	$Value$
DC link Voltage (V_{dc})	700 V
R_s	3.7 Ω
R_r	2.459 Ω
L_m	329 mH
L_{ls}	17.34 mH
L_{lr}	17.34 mH
p	4.0
ω_{nom}	1435 rpm
T_{nom}	10 $N-m$
J	0.0106 Kg/m^2

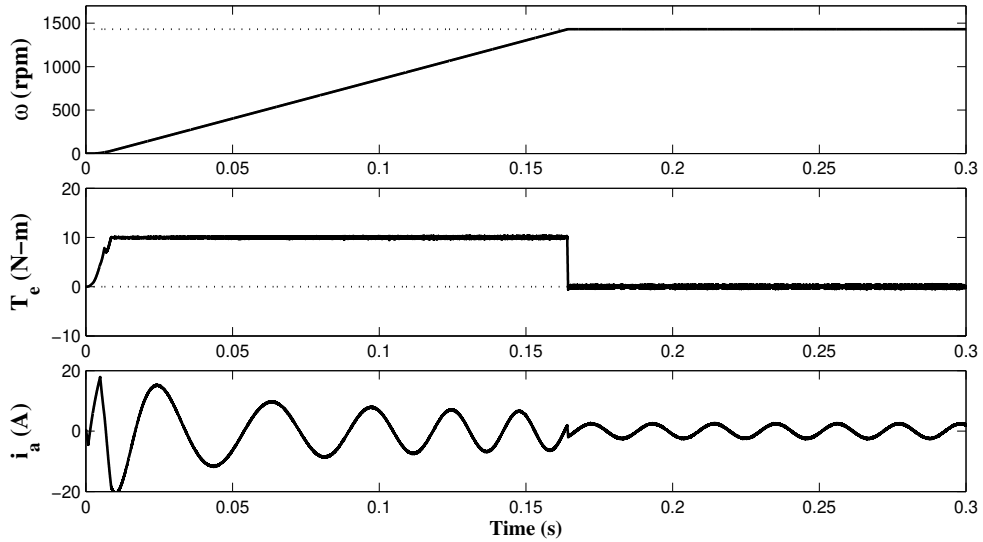

Fig. 3.4: Simulations results: torque, flux and stator current waveforms of PCC at the start.

state are shown in **Fig. 3.4** to Fig. 3.9.

From these figures, it is clear that both methods have good and behave similarly. The PCC method has a slightly better current response but the torque ripples with the PTC method are lower in comparison to that of the PCC method. The performances in the whole speed range are also investigated. The motor rotates from positive nominal speed to negative nominal speed. During this dynamic conditions (speed - reversal), the measured speed, the torque, and the stator current are observed. The results for the two methods are depicted in Fig. 3.10 and Fig. 3.11 respectively.

It is clear that both methods have very similar responses. Both of them have almost the same settling time of 310 ms to complete this speed reversal process due to the same external speed PI parameters. The torque ripples of the PTC method are slightly lower than those of the PCC method. From these results, we can conclude that two methods can work well in the whole speed range and have good behaviors with full load under steady states.

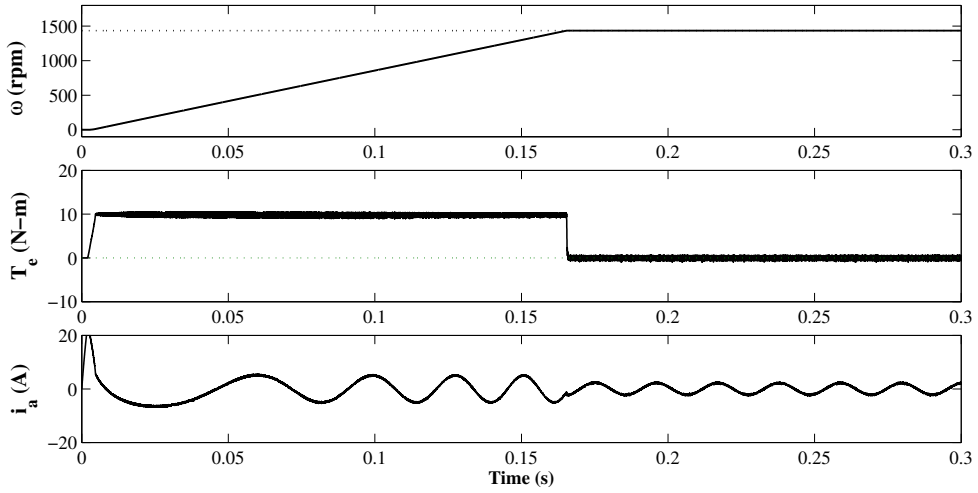

Fig. 3.5: Simulations results: torque, flux and stator current waveforms of PTC at the start.

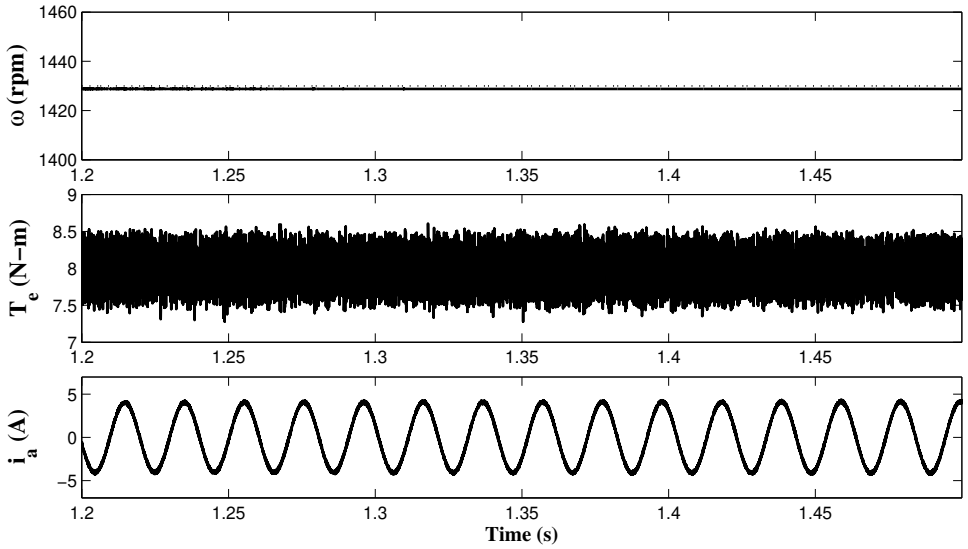

Fig. 3.6: Simulations results: torque, flux and stator current waveforms of PCC in steady state.

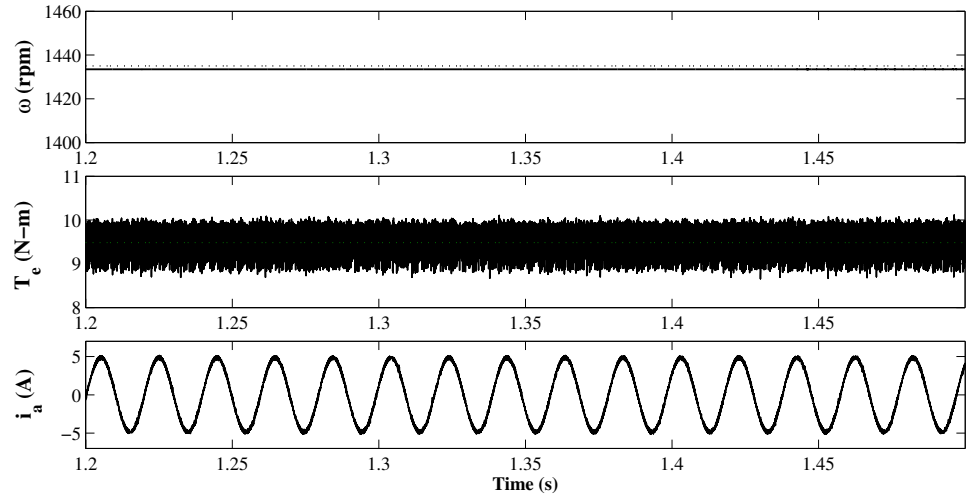

Fig. 3.7: Simulations results: torque, flux and stator current waveforms of PTC in steady state.

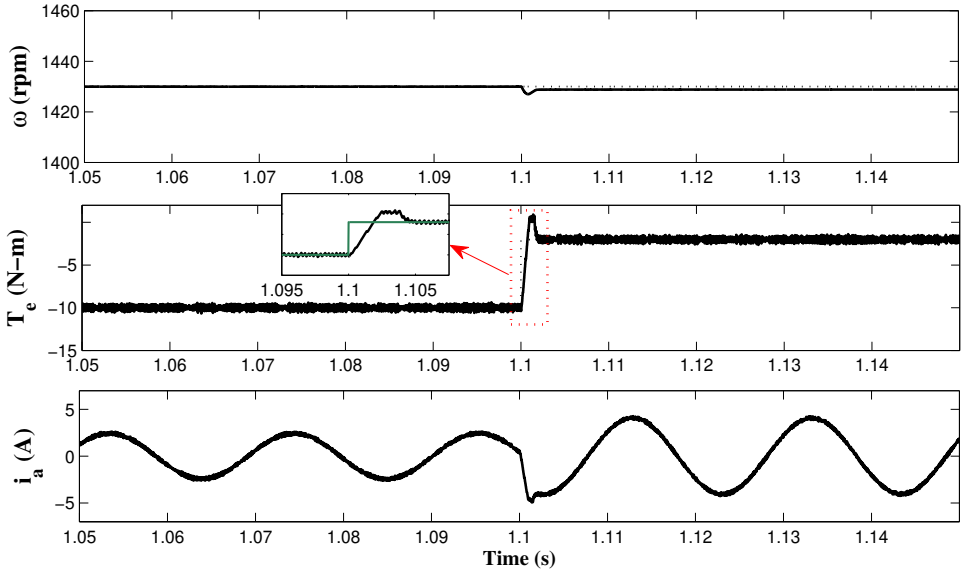

Fig. 3.8: Simulations results: torque, flux and stator current waveforms of PCC in transient state.

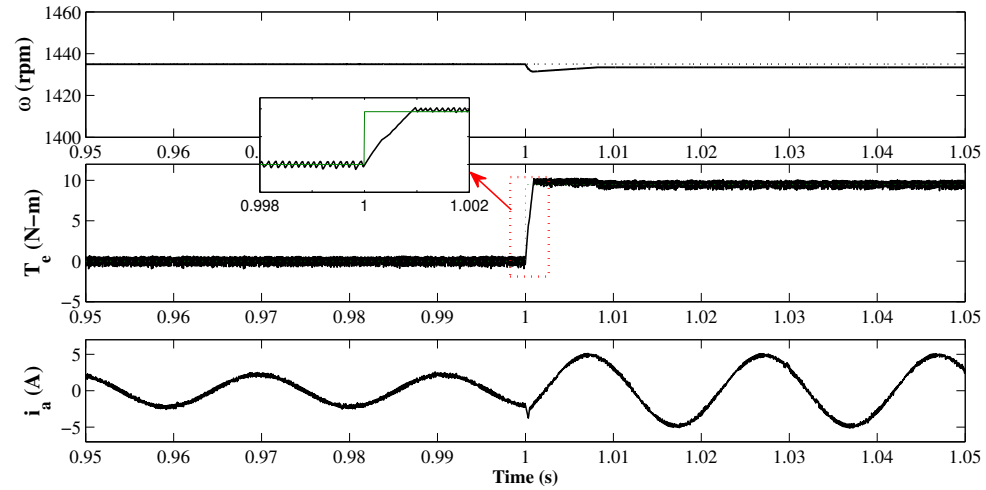

Fig. 3.9: Simulations results: torque, flux and stator current waveforms of PTC in transient state.

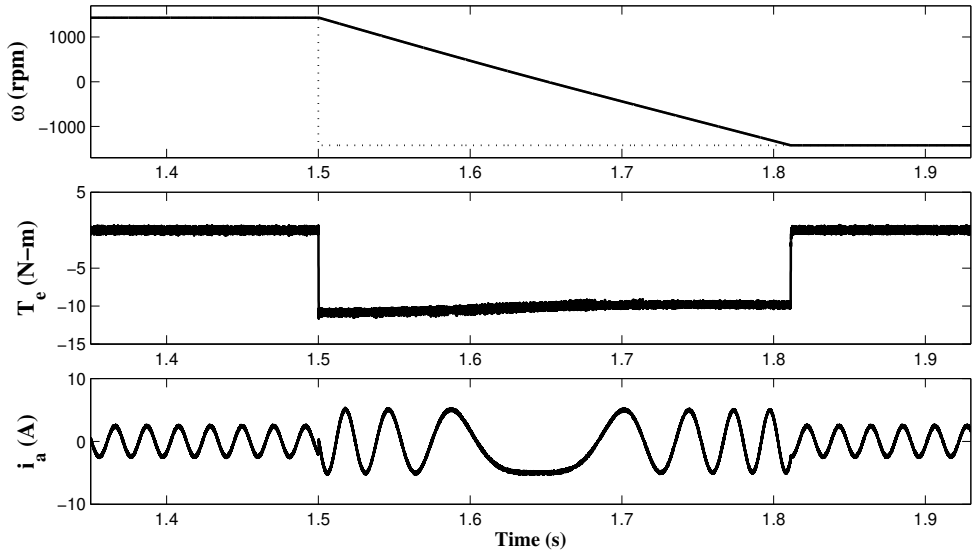

Fig. 3.10: Simulations results: torque, flux and stator current waveforms of PCC during a full speed reversal maneuver.

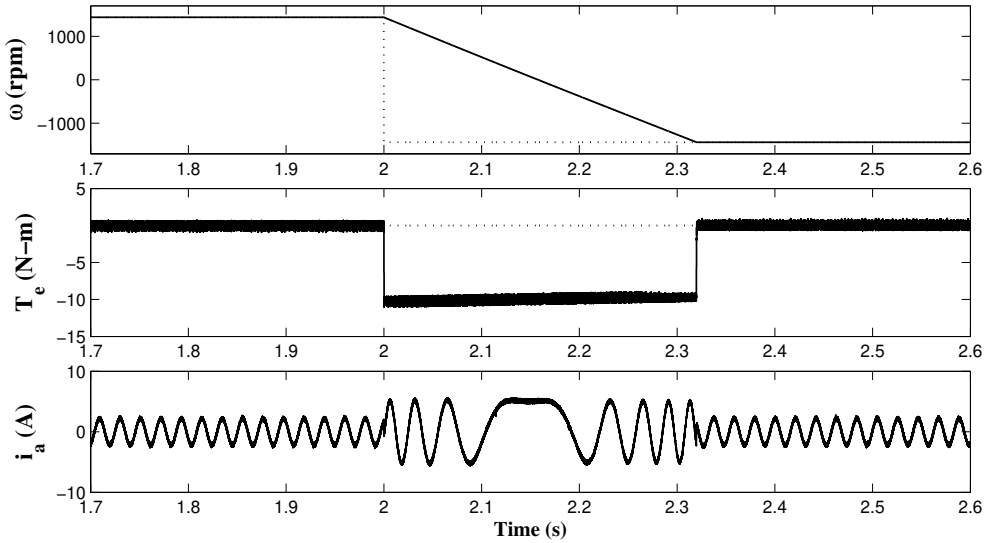

Fig. 3.11: Simulations results: torque, flux and stator current waveforms of PTC during a full speed reversal maneuver.

3.3.2 Implementation Analysis

The PTC and PCC methods are simulated and compared, and the results are shown in this report. In this section, the details of the comparisons are discussed. They have many features in common. Both the PTC and PCC methods belong to the FCS-MPC, and both have intuitive concepts and straightforward implementations compared to the FOC method. However, in the PCC method, Park transformation is a must, which requires the calculation of the rotor flux angle. Therefore, the PTC method is a little simpler than the PCC method. Neither method requires an inner current PI controller, and they each have the merit of the absence of a modulator, which leads to fast dynamics but suffer from variable switching frequency. Due to the merits of MPC, the cost functions are very flexible and the system constraints are very easy to include in both the PCC and PTC methods.

The two different MPC methods simulated in this report have some different results. Regarding the calculation efforts, the PCC method has a lower burden because its algo-

rithm calculates only current equations, but the PTC method calculates the stator flux, the stator currents and the torque for all feasible voltage vectors. Even the PCC method needs Park and inverse park transformations, but this calculation time is insignificant compared to the execution of the predictions and cost function. In this test, a two-level voltage source inverter is used that has seven different voltage vectors. If a multilevel inverter is used, the PCC algorithm can greatly reduce the calculation time. Therefore, the conclusion can be drawn that the PCC method can handle higher sampling frequencies more easily than the PTC method.

CHAPTER 4

Modulated Model Predictive Control

4.1 Introduction

Due to technological advances and emergence of faster and powerful microcontrollers that are capable of handling complex calculations, predictive control has emerged as an alternative control method for power converter in various applications. This technique is also very intuitive and is easy to implement. It also performs well despite numerous restrictions. The technique can compensate for downtime or nonlinearities in the system, offer a flexible control method and is easily extendible for different applications. However, there are some disadvantages in this type of control method. One of the major drawbacks of this method is that the control can choose only from a limited number of valid switching states due to the absence of a modulator. This generates noise as well as large voltage and current ripples.

Different solutions have been proposed in [30], [31] and [32] which allow the operation at fixed switching frequency. However, these result in complicated expressions for the switching time calculations and they are not very intuitive due to the added complications of introducing other objectives into the cost function. In order to solve these problems, a new solution is proposed in this theses which allows operation at a fixed switching frequency while maintaining the advantages of predictive control. A faster algorithm to the already proposed method is also discussed later. The proposed method describes the implementation of space vector modulation (SVM) with a linear PI controller, using a suitable modulation scheme in the cost function minimization of the

predictive algorithm for a selected number of switching states. This will generate the duty cycles for two active vectors and the two zero vectors which are applied to the converter using a given switching pattern.

4.2 Topology and mathematical model of the Voltage Source Inverter

The topology of a voltage source inverter (VSI) is already shown in Fig. 3.1. One restriction for the correct operation of this converter is to ensure that the two switches in each leg must operate in a complementary mode in order to avoid shortcircuit of the DC-source. As a result, only eight possible switching states are allowed from which the line-to-line output voltages and DC-link current are generated as shown in **Table 4.1** and **Table 4.2**.

The DC-link current i_{dc} can be determined as a function of the inverter switches and

Table 4.1: Valid switching states of the VSI.

$State$	S_a	S_b	S_c	$\overline{S_a}$	$\overline{S_b}$	$\overline{S_c}$
1	1	0	0	0	1	1
2	1	1	0	0	0	1
3	0	1	0	1	0	1
4	0	1	1	1	0	0
5	0	0	1	1	1	0
6	1	0	1	0	1	0
7	1	1	1	0	0	0
8	0	0	0	1	1	1

the output currents i as:

$$i_{dc} = [S_1\ S_3\ S_5]\ i \tag{4.1}$$

Table 4.2: Output line to line voltages and currents of the VSI.

$State$	v_{ab}	v_{bc}	v_{ca}	i_{dc}
1	v_{dc}	0	-v_{dc}	i_a
2	0	v_{dc}	-v_{dc}	i_a + i_b
3	-v_{dc}	v_{dc}	0	i_b
4	-v_{dc}	0	-v_{dc}	i_b + i_c
5	0	-v_{dc}	v_{dc}	i_c
6	v_{dc}	-v_{dc}	0	i_a + i_c
7	0	0	0	0
8	0	0	0	0

The output voltage can be defined as a function of the inverter switches and the DC-link voltage v_{dc} as:

$$v = \begin{bmatrix} S_1 \\ S_3 \\ S_5 \end{bmatrix} v_{dc} \tag{4.2}$$

From Fig. 3.1, the continuous model of the converter is:

$$v = L\frac{di}{dt} + Ri \tag{4.3}$$

From (4.3) it is possible to obtain a discrete time model, assuming that the variables are constant during a sampling time T_s:

$$i^{k+1} = (1 - \frac{RT_s}{L})i^k + \frac{T_s}{L}v^k \tag{4.4}$$

4.3 Basic modulated model predictive control algorithm

In space vector modulation (SVM), it is possible to define each available vector for the VSI in the $\alpha - \beta$ plane as shown in Fig. 3.1. It is possible to define six sectors which

are falling between two adjacent vectors,for example, sector 1 falls between vector v_1 and vector v_2. These vectors correspond to the voltage generated by switching state 1 and switching state 2, respectively, based on (4.2) and **Table 4.1**. The proposed control method is shown in Fig. 4.1 and is the same idea as the classical predictive control

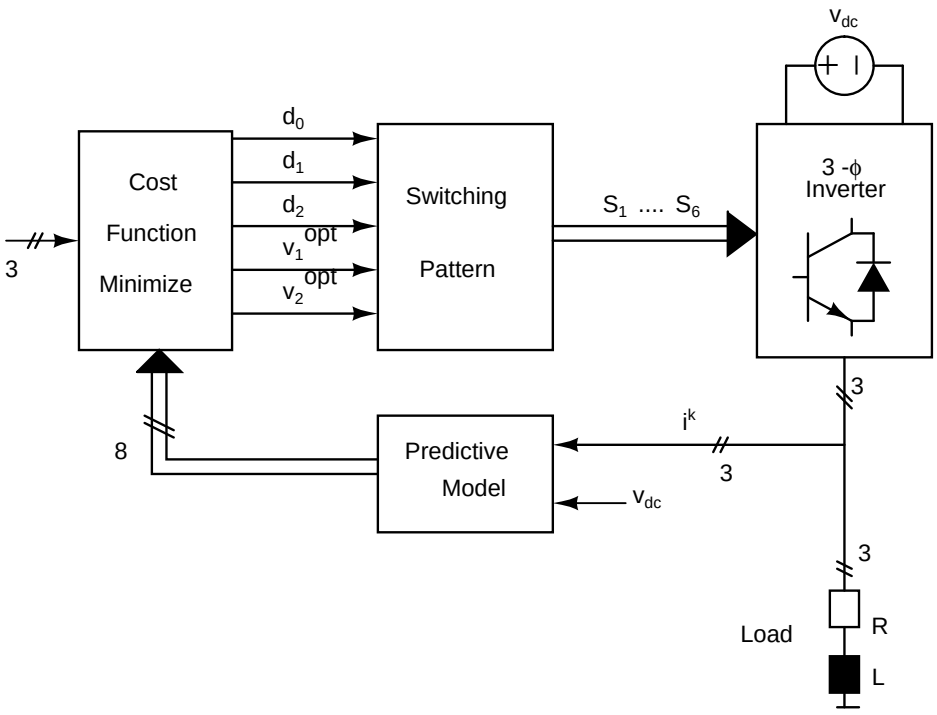

Fig. 4.1: Proposed modulated model predictive current control scheme

method as it uses the same prediction of the load current indicated in (4.4).
Moreover the proposed technique evaluates the prediction of the two active vectors that lie in each sector at every sampling time and evaluates the cost function separately for each prediction. The cost function g is evaluated for each case and is the same as the one considered for the classical predictive method. For example, in sector 1, the first prediction i.e the cost function g_1 is evaluated for vector v_1 and the second prediction and cost function g_2 is evaluated for vector v_2. Each prediction is evaluated based on (4.4) and the only change is in respect to the calculation of the load voltage v. The duty

cycles for the two active vectors are calculated by solving:

$$\begin{aligned} d_0 &= K/g_0 \\ d_1 &= K/g_1 \\ d_2 &= K/g_2 \\ d_0 + d_1 + d_2 &= T_s \end{aligned} \tag{4.5}$$

where d_0 correspond to the duty cycle of a zero vector which is evaluated only one time and K is a constant. By solving the system of equations in (4.5), it is possible to obtain the expression for K and the expressions for the duty cycles for each vector can be written as:

$$\begin{aligned} d_0 &= T_s g_1 g_2/(g_0 g_1 + g_1 g_2 + g_0 g_2) \\ d_1 &= T_s g_0 g_2/(g_0 g_1 + g_1 g_2 + g_0 g_2) \\ d_2 &= T_s g_0 g_1/(g_0 g_1 + g_1 g_2 + g_0 g_2) \end{aligned} \tag{4.6}$$

With the afore mentioned expressions, the new cost function, which is evaluated at every sampling time becomes

$$g(k+1) = d_1 g_1 + d_2 g_2 \tag{4.7}$$

The two vectors that minimize this cost function are selected and applied to the converter in the next sampling time. After obtaining the duty cycles and selecting the two optimal vectors to be applied, a switching pattern procedure, such as the one shown in Fig. 4.2, is adopted with the goal of applying the two active vectors and one zero vector (using two zero states). The switching pattern procedure for the modified method is shown in Fig. 4.3.

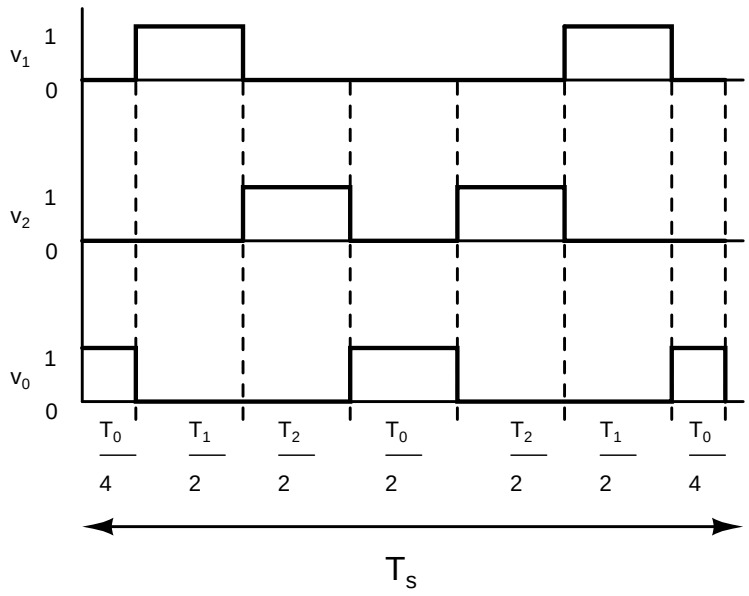

Fig. 4.2: Switching pattern for the optimal vectors

4.4 Proposed algorithm change

While the above method is the most conventional form of modulated model predictive control implementation, it's approach is quite time consuming. From the above algorithm, it is evident that in each sampling time period, the duty cycles have to be calculated for each sector and then $g(k+1)$ also has to be calculated for each of the 6 sectors before comparison of the minimal value of the cost function to be used for the next cycle. This process of over calculation of each parameter served as the motivation and need to identify a better optimized algorithm which outputs the same result but with a faster approach. In this algorithm, the six different values of the cost function are calculated for each sector and the minimal of those 6 are found. This minimal value is then used to calculate the duty ratios and the cost function for the next sampling period.

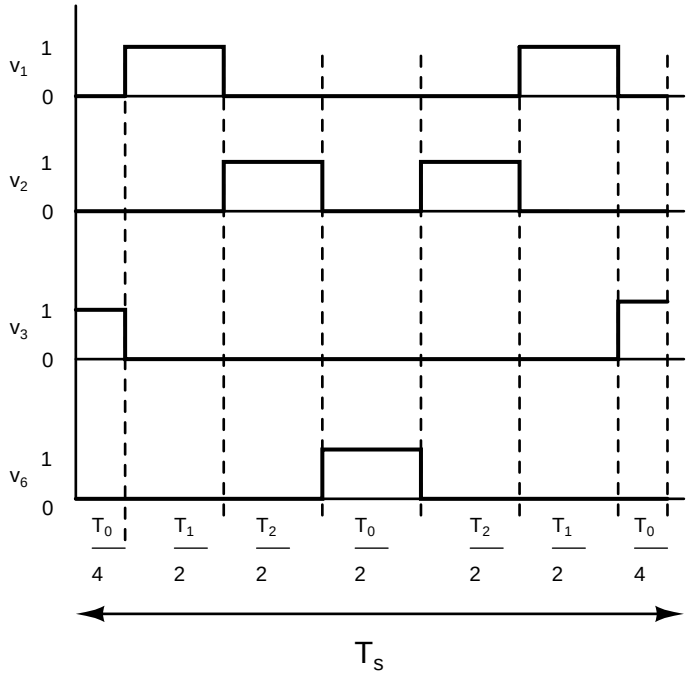

Fig. 4.3: Switching pattern for the optimal vectors of the modified method

The equation form are mentioned below:

$$\begin{aligned} G_1 &= g_1 g_2 \\ G_2 &= g_2 g_3 \\ G_3 &= g_3 g_4 \\ G_4 &= g_4 g_5 \\ G_5 &= g_5 g_6 \\ G_6 &= g_6 g_1 \end{aligned} \tag{4.8}$$

where G is the product of the cost functions calculated from the voltage space vectors. The minimum of the 6 $G's$ is then selected and they become the respective g_1 and g_2 for the current sampling period. The g_0 remains the same for all the 6 $G's$ and hence can be used directly with the respective g_1 and g_2 into (4.6) and (4.7). As an example,

suppose in the present sampling period, if G_4 has the minimum value among all the six, this would mean that g_4 would replace g_1 and g_5 replaces g_2 in (4.6) and (4.7). This algorithm bypasses the entire need to calculate the different values from (4.5) to be used in (4.6) before the minimal value is found and then replaced in (4.7). Thus, the proposed algorithm loops over only once to get to the final cost function as compared to the original algorithm that uses 2 loops. The mathematical proof for the proposed algorithm is presented in Appendix of the report.

4.5 Implementation and Results

In order to validate the effectiveness of the proposed methods, simulation results are carried out in steady and transient conditions for both the basic and proposed methods. These results are then compared with the results obtained with the classical predictive control implementation. The simulation parameters are the same as given in **Table 3.1**.

4.5.1 Simulation results in Steady State

Fig. 4.4 show the simulation results in steady state for the classical predictive controller implementation. Fig. 4.5 and Fig. 4.6 show the same results but for the basic and proposed modulated model predictive controller algorithms respectively. In all the cases, the current posses a peak value of 5 A and with a reference frequency of 50 Hz is established.

It is observed that the load current ripples for the basic and proposed modulated model predictive schemes are slightly lower than the classical predictive method. This is also observed from the load voltage plots for the 2 schemes, in comparison to the load voltage plot of the classical predictive model.

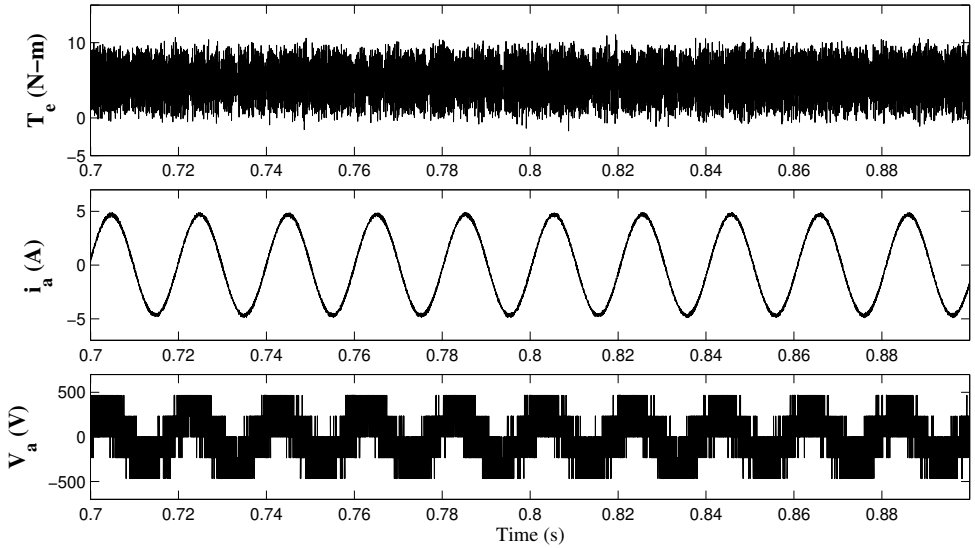

Fig. 4.4: Simulation results of measured load current and load voltage in the classical predictive control method in steady state condition.

4.5.2 Results in Transient State

In order to demonstrate the performance of the proposed strategies in terms of dynamic response, transient state analysis is necessary. Fig. 4.7 shows results for the classical predictive method and Fig. 4.8 shows the same results for the basic M^{2}PC method. Fig. 4.9 shows similar results but with the proposed algorithm. A step change in the load current from 5 A to 3.5 A is applied at instant t = 1 s. In all the cases, a very good dynamic response is observed and again lower load current ripple is observed for the proposed predictive controller scheme.

One interesting issue that is observed for the classical predictive controller is a reduction in the switching frequency, when a lower load current reference is applied and thus a variable switching frequency is present. Consequently, for the basic and proposed

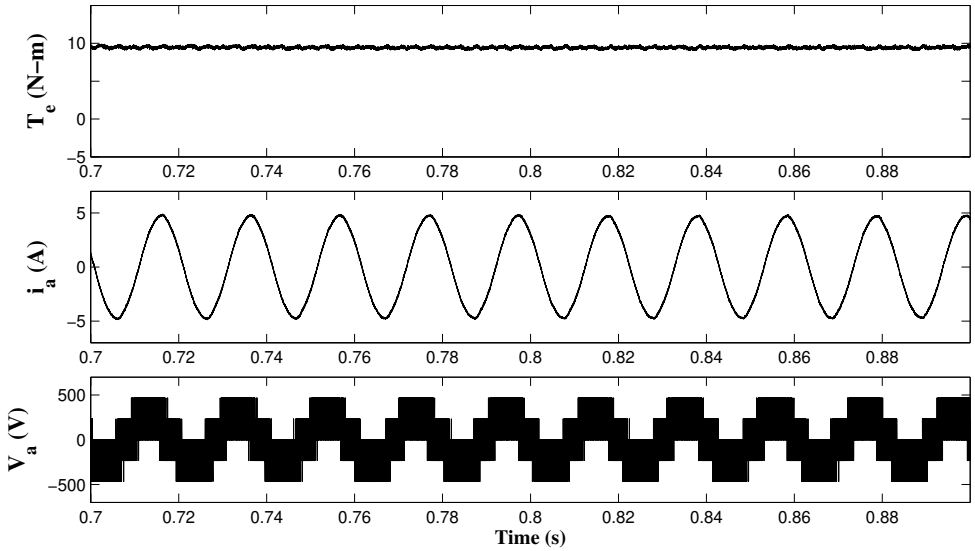

Fig. 4.5: Simulation results of measured load current and load voltage in the basic modulated model predictive control method in steady state condition.

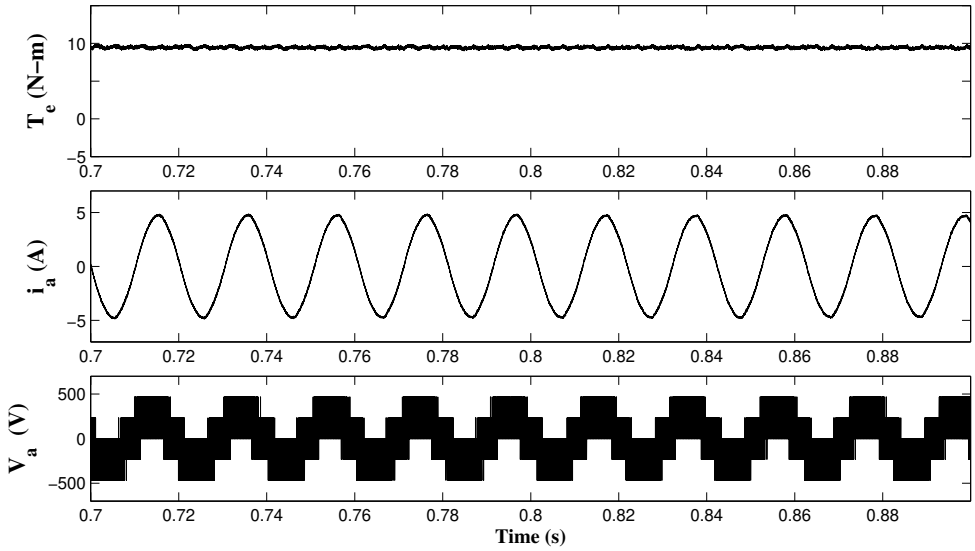

Fig. 4.6: Simulation results of measured load current and load voltage in the proposed modulated model predictive control method in steady state condition.

predictive scheme, a constant switching frequency is observed, despite of the load

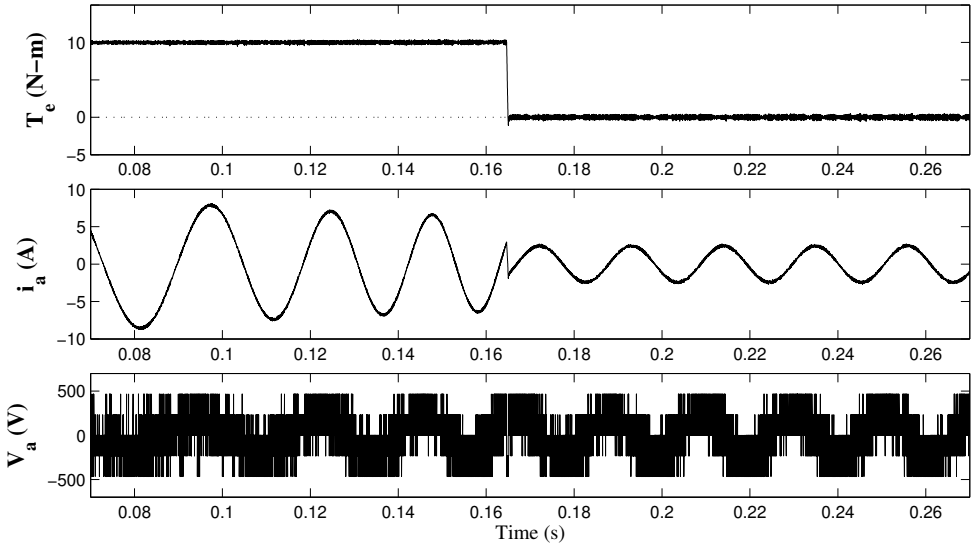

Fig. 4.7: Simulation results of measured load current and load voltage in the classical predictive control method in transient condition.

current reference applied.

4.5.3 Implementation Analysis

In the FS-MPC controller, as the control is updated at every sampling time interval (which means that only one output voltage vector is applied during the whole sampling period), the resulting switching frequency becomes variable where the maximum switching frequency occurs for a reference that is equivalent to a duty cycle of 0.5.This decreases as the reference moves away from 0.5. Thus, in order to have a high switching frequency for every reference, the control algorithm has to be evaluated at a higher rate than the switching frequency. Additionally, it is necessary to select a high sampling time in order to minimize the variations in inverter switching frequency and enable it to follow the average switching frequency. With the proposed M^2PC method, it is possible

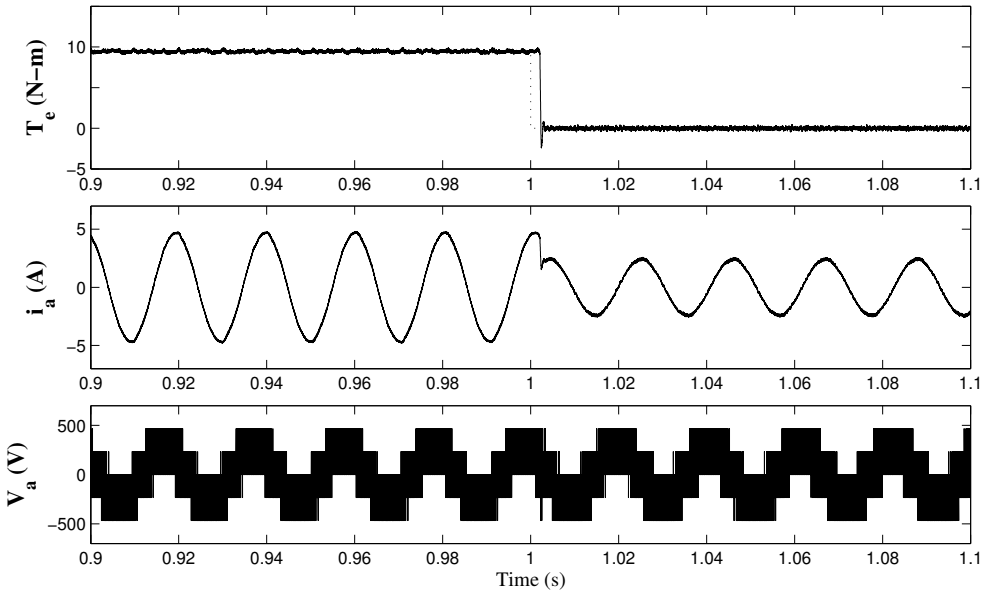

Fig. 4.8: Simulation results of measured load current and load voltage in the basic modulated model predictive control method in transient condition.

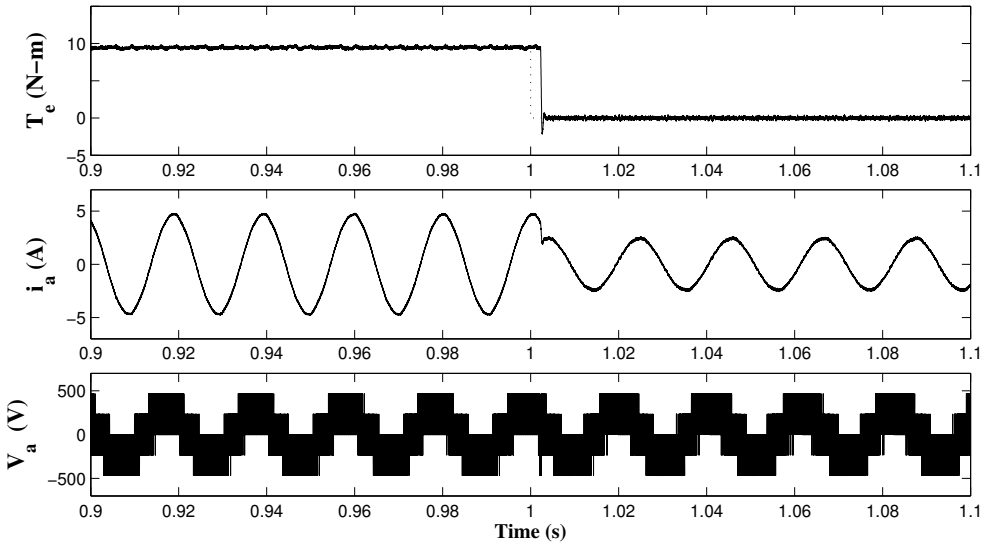

Fig. 4.9: Simulation results of measured load current and load voltage in the proposed method of modulated model predictive control method in transient condition.

to eliminate the main disadvantage of predictive control which is the variable switching frequency. By considering a M^2PC scheme, it is possible to consider the use of two active vectors and the two zero vectors during each sampling period. The operation at fixed switching frequency produces less current and torque ripple and a more predictable harmonic spectrum, which reflects in an improvement in the performance of the motor drive system.

CHAPTER 5

Conclusion

This report discusses various speed control strategies of IM drives . Initially classical open-loop strategies were discussed like the v/f control, slip recovery etc. It was then figured that the deviation between the predicted and the actual behaviour is something that has to be accounted for but these strategies don't deal with them. This gave rise to the need of a better and more advanced control method, called the predictive control method.

Various predictive control methods were discussed like the hysteresis control, the deadbeat control etc. Each of them have their advantages and disadvantages, but the one that stood out of all the remaining was the model predictive control (MPC) which exhibits superiority as that of the FOC strategy. The report demonstrates that predictive control is a powerful and flexible concept for designing controllers. It presents several advantages that make it suitable for the control of power converters and motor drives. The use of the available information of the system to decide the optimal actuation helped achieve fast dynamics, by including the nonlinearities and restrictions of the system and avoids the cascaded structure. It is also possible to take advantage of the discrete nature of the power converters and choose from the possible switching states the optimal solution according to the minimization of a predefined cost function.This led to the development of two very prominent predictive control methods, the PCC and PTC.

A Close evaluation was carried out between these two FS-MPC control strategies. Though both methods are direct control methods without an inner current PI controller or a modulator, the PCC method has lower calculation time than the PTC method. This advantage makes the PCC method more appropriate for applications with longer prediction

horizons. From the test results, it is clear that the PCC method and the PTC method have very good and similar performances in both steady and transient states. The PCC method. However, the PCC method is better when the currents are evaluated. The PCC method shows strong robustness with respect to the stator resistance; however, the PTC method shows much better robustness with respect to the magnetizing inductance. While this evaluation helped us gauge the basic idea of these two methods, a modulated version of the MPC is also presented in this report and it gives better and faster results whilst maintaining a fixed switching frequency.

The M^2PC was then introduced as it allows for carrying out all the operations of a converter in a fixed switching frequency whilst maintaining all the advantages of the classical finite-state model predictive control techniques such as fast dynamic response and easy inclusion of nonlinearities. As the basic algorithm presented here is tedious, a new optimized algorithm was then developed to minimize the cost function at a faster rate. Simulations results demonstrate that this is a viable alternative to avoid linear controllers and performs well in both steady and transient conditions with good tracking to its references and a reduced ripple.

APPENDIX A

APPENDIX I

A.1 Mathematical Proof for the proposed algorithm in Modulated Model Predictive Control

This section will give a mathematical proof of the optimized algorithm proposed for the modulated model predictive control. In the basic model seven values of g are obtained from g_0 to g_6 in each sampling cycle. The equations used for the basic model are:

$$\begin{aligned} d_0 &= K/g_0 \\ d_1 &= K/g_1 \\ d_2 &= K/g_2 \\ d_0 + d_1 + d_2 &= T_s \end{aligned} \tag{A.1}$$

These sets of equations are used in each sector to calculate six different values of d_0, d_1 and d_2, where d_0 correspond to the duty cycle of a zero vector which is evaluated only one time. On solving, the equations obtained will be:

$$\begin{aligned} d_0 &= T_s g_1 g_2/(g_0 g_1 + g_1 g_2 + g_0 g_2) \\ d_1 &= T_s g_0 g_2/(g_0 g_1 + g_1 g_2 + g_0 g_2) \\ d_2 &= T_s g_0 g_1/(g_0 g_1 + g_1 g_2 + g_0 g_2) \end{aligned} \tag{A.2}$$

The minimum was then evaluated and implemented in the cost function:

$$g(k+1) = d_1 g_1 + d_2 g_2 \tag{A.3}$$

From (A.1) and (A.2), the following expression for K can be obtained

$$K = T_s g_1 g_2 g_0 / (g_0 g_1 + g_1 g_2 + g_0 g_2) \tag{A.4}$$

Thus, for six different sectors, six different $K's$ are calculated. In the original method, the minimum of $g(k+1)$ is needed for the next sample, which is the same as calculating the minimum of $d_1 g_1 + d_2 g_2$. From equations (A.1), it is clear that $d_1 g_1 + d_2 g_2 = 2K$. Thus, all that is needed is to find the minimum of the various $K's$ that have been calculated. From (A.4), the expression for K is achieved. Taking the inverse of it gives:

$$\frac{1}{K} = \frac{g_0(g_1 + g_2)}{g_0 g_1 g_2} + \frac{g_1 g_2}{g_0 g_1 g_2} \tag{A.5}$$

This further simplifies to:

$$\frac{1}{K} = \frac{g_1 + g_2}{g_1 g_2} + \frac{1}{g_0} \tag{A.6}$$

Now the minimum among six $K's$ needs to be found. This would in turn imply the need to find the maximum of six $\frac{1}{K's}$. As g_0 is the same across all the six sectors in a single sampling interval, $\frac{1}{g_0}$ will not play any role in determining the maximum of $\frac{1}{K's}$.
So

$$max(\frac{1}{K}) = max(\frac{g_1 + g_2}{g_1 g_2}). \tag{A.7}$$

Now mathematically it is known that

$$g_1 g_2 >> g_1 + g_2. \tag{A.8}$$

Therefore

$$max(\frac{1}{K}) = max(\frac{1}{g_1 g_2}). \tag{A.9}$$

Which in turn implies that all that needs to be done is to find the **min ($g_1 g_2$)** for each of the six sectors, which is defined as G in Section 4.4. This would involve calculating the minimum of the product of $g's$ in each sector and use it in calculating just the final set of duty ratios and the final cost function and thus run in just one loop.

REFERENCES

[1] Neelakantha Guru, Santosh Kumar Mishra, and B. Nayak. Article: Indirect vector control of multi cage induction motor. *International Journal of Computer Applications*, 68(2):25–32, April 2013.

[2] R. A. Hamilton and G. R. Lezan. Thyristor adjustable frequency power supplies for hot strip mill run-out tables. *IEEE Transactions on Industry and General Applications*, IGA-3(2):168–175, March 1967.

[3] W. Slabiak and L. J. Lawson. Precise control of a three-phase squirrel-cage induction motor using a practical cycloconverter. *IEEE Transactions on Industry and General Applications*, IGA-2(4):274–280, July 1966.

[4] W. Shepherd and J. Stanway. An experimental closed-loop variable speed drive incorporating a thyristor driven induction motor. *IEEE Transactions on Industry and General Applications*, IGA-3(6):559–565, Nov 1967.

[5] Jong Woo Choi, Sung Il Yong, and Seung Ki Sul. Inverter output voltage synthesis using novel dead time compensation. In *Applied Power Electronics Conference and Exposition, 1994. APEC '94. Conference Proceedings 1994., Ninth Annual*, pages 100–106 vol.1, Feb 1994.

[6] R. B. Sepe and J. H. Lang. Inverter nonlinearities and discrete-time vector current control. *IEEE Transactions on Industry Applications*, 30(1):62–70, Jan 1994.

[7] K. Koga, R. Ueda, and T. Sonoda. Achievement of high performances for general

purpose inverter drive induction motor system. In *Conference Record of the IEEE Industry Applications Society Annual Meeting,*, pages 415–425 vol.1, Oct 1989.

[8] Y. Xue, X. Xu, T. G. Habetler, and D. M. Divan. A low cost stator flux oriented voltage source variable speed drive. In *Conference Record of the 1990 IEEE Industry Applications Society Annual Meeting*, pages 410–415 vol.1, Oct 1990.

[9] K. Koga, R. Ueda, and T. Sonoda. Constitution of v/f control for reducing the steady state speed error to zero in induction motor drive system. In *Conference Record of the 1990 IEEE Industry Applications Society Annual Meeting*, pages 639–646 vol.1, Oct 1990.

[10] P. Cortes, M. P. Kazmierkowski, R. M. Kennel, D. E. Quevedo, and J. Rodriguez. Predictive control in power electronics and drives. *IEEE Transactions on Industrial Electronics*, 55(12):4312–4324, Dec 2008.

[11] A. Khambadkone and J. Holtz. Low switching frequency and high dynamic pulsewidth modulation based on field-orientation for high-power inverter drive. *IEEE Transactions on Power Electronics*, 7(4):627–632, Oct 1992.

[12] M. Depenbrock. Direct self-control (dsc) of inverter-fed induction machine. *IEEE Transactions on Power Electronics*, 3(4):420–429, Oct 1988.

[13] I. Takahashi and T. Noguchi. A new quick-response and high-efficiency control strategy of an induction motor. *IEEE Transactions on Industry Applications*, IA-22(5):820–827, Sept 1986.

[14] R. E. Betz, S. J. Henriksen, B. J. Cook, and T. Summers. Practical aspects of instantaneous power control of induction machines. In *Conference Record of the 2001 IEEE Industry Applications Conference. 36th IAS Annual Meeting (Cat. No.01CH37248)*, volume 3, pages 1771–1778 vol.3, Sept 2001.

[15] G. H. Bode, Poh Chiang Loh, M. J. Newman, and D. G. Holmes. An improved robust predictive current regulation algorithm. *IEEE Transactions on Industry Applications*, 41(6):1720–1733, Nov 2005.

[16] H. Abu-Rub, J. Guzinski, Z. Krzeminski, and H. A. Toliyat. Predictive current control of voltage-source inverters. *IEEE Transactions on Industrial Electronics*, 51(3):585–593, June 2004.

[17] Y. Abdel-Rady, I. Mohamed, and E. F. El-Saadany. A novel deadbeat current control scheme with an adaptive self-tuning load model for a three-phase pwm-vsi. In *2007 IEEE Power Electronics Specialists Conference*, pages 36–42, June 2007.

[18] Y. A. R. I. Mohamed and E. F. El-Saadany. Robust high bandwidth discrete-time predictive current control with predictive internal model x2014;a unified approach for voltage-source pwm converters. *IEEE Transactions on Power Electronics*, 23(1):126–136, Jan 2008.

[19] Y. A. R. Ibrahim and E. F. El-Saadany. An adaptive grid-voltage sensorless interfacing scheme for inverter-based distributed generation. In *2008 IEEE Power and Energy Society General Meeting - Conversion and Delivery of Electrical Energy in the 21st Century*, pages 1–10, July 2008.

[20] P. Mattavelli, G. Spiazzi, and P. Tenti. Predictive digital control of power factor preregulators with input voltage estimation using disturbance observers. *IEEE Transactions on Power Electronics*, 20(1):140–147, Jan 2005.

[21] P. Mattavelli. An improved deadbeat control for ups using disturbance observers. *IEEE Transactions on Industrial Electronics*, 52(1):206–212, Feb 2005.

[22] J. D. Barros and J. F. Silva. Optimal predictive control of three-phase npc multilevel converter for power quality applications. *IEEE Transactions on Industrial Electronics*, 55(10):3670–3681, Oct 2008.

[23] I. Takahashi and T. Noguchi. A new quick-response and high-efficiency control strategy of an induction motor. *IEEE Transactions on Industry Applications*, IA-22(5):820–827, Sept 1986.

[24] I. Takahashi and Y. Ohmori. High-performance direct torque control of an induction motor. *IEEE Transactions on Industry Applications*, 25(2):257–264, Mar 1989.

[25] S. A. Davari, D. A. Khaburi, and R. Kennel. An improved fcs x2013;mpc algorithm for an induction motor with an imposed optimized weighting factor. *IEEE Transactions on Power Electronics*, 27(3):1540–1551, March 2012.

[26] C. A. Rojas, J. Rodriguez, F. Villarroel, J. R. Espinoza, C. A. Silva, and M. Trincado. Predictive torque and flux control without weighting factors. *IEEE Transactions on Industrial Electronics*, 60(2):681–690, Feb 2013.

[27] Jose Rodriguez, Marian P. Kazmierkowski, Jose R. Espinoza, Pericle Zanchetta, Haitham Abu-Rub, Hector A. Young, and Christian A. Rojas. State of the art of finite control set model predictive control in power electronics. *IEEE Transactions on Industrial Informatics*, 9(2):1003–1016, 5 2013.

[28] J. Rodriguez, J. Pontt, C. A. Silva, P. Correa, P. Lezana, P. Cortes, and U. Ammann. Predictive current control of a voltage source inverter. *IEEE Transactions on Industrial Electronics*, 54(1):495–503, Feb 2007.

[29] M. Nemec, D. Nedeljkovic, and V. Ambrozic. Predictive torque control of induction machines using immediate flux control. *IEEE Transactions on Industrial Electronics*, 54(4):2009–2017, Aug 2007.

[30] P. Antoniewicz and M. P. Kazmierkowski. Virtual-flux-based predictive direct power control of ac/dc converters with online inductance estimation. *IEEE Transactions on Industrial Electronics*, 55(12):4381–4390, Dec 2008.

[31] Jiabing Hu and Z.Q. Zhu. Improved voltage-vector sequences on dead-beat predictive direct power control of reversible three-phase grid-connected voltage-source converters. 28:254–267, 01 2013.

[32] A. Llor, M. Fadel, A. Ziani, M. Rivera, and J. Rodriguez. Geometrical approach for a predictive current controller applied to a three-phase two-level four-leg inverter. In *IECON 2012 - 38th Annual Conference on IEEE Industrial Electronics Society*, pages 5049–5056, Oct 2012.